Full-Scale Prototype Testing and Manufacturing and Installation Plans for New Scour-Vortex-Prevention scAUR™ and VorGAUR™ Products for a Representative Scour-critical Bridge

IDEA Program Final Report

NCHRP- IDEA Project 162

Prepared for the IDEA Program
Transportation Research Board
The National Academies

Roger L. Simpson, Ph.D., P.E., Principal Investigator
Applied University Research, Inc.
July 13, 2013

Acknowledgments

This report was prepared under NCHRP-IDEA Project 162 by AUR, Inc. Funding was provided by the NCHRP-IDEA Program and by AUR, Inc. Dr. Inam Jawed of the NCHRP-IDEA Program was always helpful in the administration and review of this project. Mr. Kendal Walus, P.E.,Virginia Department of Transportation (VDOT) State Structure and Bridge Engineer, Mr. Mark W. Richardson, P. E., Administrator, Bridge Design Bureau, and Mr. Timothy S. Mallette, PLS, P.E., Hydraulics Engineer, both of New Hampshire DOT, and Mr. David P. Hohmann, P.E., Bridge Division Director, Texas DOT endorsed this project.

The NCHRP-IDEA Project Expert Advisory Committee was composed of the Chairman, Dr. Edward J. Hoppe, Ph.D., P. E., Senior Research Scientist, Geotechnical Engineering, Virginia Department of Transportation (VDOT) Virginia Center for Transportation Innovation and Research (VCTIR) in Charlottesville, Virginia, Mr. John H. Matthews, P. E., VDOT Assistant State Hydraulics Engineer, Engineering Services Section Manager, and Mr. John G. Delphia, P.E., Texas DOT, Bridge Division, Geotechnical Branch. This committee provided useful suggestions and feedback on many related issues, such as scour-critical candidate bridges for implementation, manufacturing methods, and the model flume tests.

The principal investigator was assisted in the work by Dr. Gwibo Byun and Mr. Edmund Mueller of AUR, Inc. Dr. Q. Q. Tian and Dr. J. A. DeMoss of AUR, Inc. made early contributions to the computational fluid dynamics work. Mr. Dale Gallimore of the AUR, Inc staff constructed the full-scale test model and modified the AUR flume equipment for these tests.

The full-scale tests in the University of Iowa Institute of Hydraulic Research (IIHR) Environmental Flow Facility were assisted by Mr. Troy Lyons, P.E. and many IIHR laboratory staff. Andrew Craig, P. E., Timothy Houser, and Brandon Barquist of IIHR witnessed the results of these full-scale tests.

Table of Contents

EXECUTIVE SUMMARY

Local scour of bridge piers and abutments is one of the most common causes of highway bridge failures *(1)*. All currently used countermeasures are temporary and do not prevent the cause of scour – discrete large-scaled vortices formed by flow separations and recirculations from the underwater structures, which are shown in Figure ES.1 below. These large-scaled vortices bring higher velocity water down to the river bed and cause scour. Using the knowledge of how to prevent the formation of discrete vortices, prior to this IDEA project AUR developed, proved using model-scale tests, and patented new local-scouring-vortex-prevention products (scAUR™ as US Patent No. 8,348,553 and VorGAUR™ as US Patent No. 8,434,723) shown in Figure ES.2. These products prevent the near-free-surface higher velocity water from going down to the river bottom and cause scour. These products keep the lower velocity water near the river bed. These are practical long-term cost-effective permanent solutions to the bridge pier and abutment local scour problem, no matter what types and sizes of soil and rocks surround the pier or abutment. The payoffs for practice that were identified by that earlier work are:

1. **Permanently prevent the formation of local scouring vortical flows due to flow separation** around bridge piers and abutments of any width to length ratio that cause local scour for any size or scale bridge pier or abutment.
2. **Permanently prevent local scour**, even at large angles of stream crossflow or swirling flow due to river bends.
3. **Much lower present value of present and future scour mitigation costs** as compared to current approaches.
4. **Lower drag force, flow blockage, water level, and over-topping frequencies on bridges during flood conditions, for any water level or turbulence level.**
5. **Debris accumulation prevention and pier and abutment protection from impact loads because of the streamlined flow without a horseshoe vortex, which deflects objects and debris away from the underwater structure.**
6. **High quality proven-technology prefabricated stainless steel or cast concrete components** for quality control and rapid installation.
7. **More stability for the soil and rocks surrounding the piers and abutments.**
8. **100 year or more lifetimes and longer bridge life.**

In this current NCHRP Project, further work was done to expand knowledge of and confidence in these products for scour prevention in practical applications. This work included (a) further computational work on the effects of pier size or scale and model flume tests for (b) other sediments, (c) other abutment designs, and (d) a foundation leading edge ramp with scAUR™ to prevent foundation scour due to open bed scour conditions. Full-scale prototypes of these proven products were constructed and tested.

In preparation for future use, work was done to advance the manufacturing and installation processes for cost-effective full-scale scAUR™ and VorGAUR™ products on at least one pier and one abutment for a selected scour-critical bridge in Virginia. Based on the candidate bridge criteria of traffic volume, age, number of spans, scour critical rating, and the availability of river stream-flow data, the merits of five Virginia bridges were considered in detail and the Route 360 westbound bridge over the Appomattox River is recommended to Virginia DOT.

Since all earlier verification of scAUR™ and VorGAUR™ products was done at model scale, some research here focused on full-scale performance of these concepts. Reynolds number and bridge pier and abutment size effects on the flow were examined using a well-proven computational fluid dynamics (CFD) code. Results for model and full-scale piers show that the scAUR™ fairing is effective in preventing scour producing vortices at both model and full scale. Based on the past published work on scour and the experience of AUR *(2,3,4)*, more physical evidence and insights support the idea that these scour-vortex-preventing devices will work better at full scale than model scale. Scouring forces on river bed materials are produced by pressure gradients and turbulent shearing stresses, which are instantaneously unsteady. At higher Reynolds numbers and sizes, pressure gradients and turbulent fluctuation stresses are lower than at model scale, so scour at the same flow speed is lower. In addition, these results show that the smooth flow over the pier produces lower flow blockage than a pier without the scAUR™ shape because low velocity swirling high blockage vortices are absent. As a result, water moves around a pier or abutment faster above the river bed, producing a lower water level at the bridge and lower over-topping frequencies on bridges during flood conditions for any water level when no discrete vortices are present. **Work by others *(5,6,7)* supports the conclusion that scour predictive equations, developed largely from laboratory data, overpredict scour on full-scale underwater structures. Thus, the scAUR™ and VorGAUR™ will work just as well or better in preventing the scouring vortices and any scour at full scale as at the proven model scale.** Other CFD by AUR that is not reported here, shows that scAUR™ and VorGAUR™ products also prevent scouring vortices around bridge piers downstream of bending rivers.

Since all earlier model flume studies had used a single-size-range of pea gravel, data on the performance of these scAUR™ and VorGAUR™ products with several smaller size sediments at model scale were obtained in the AUR

flume. Data from published sources suggested that model scale tests be conducted for *t/d50* > 50, where *t/d50* is the ratio of pier width to median sediment grain diameter. AUR used values of 38.1 < *t/d50* < 64.6, as well as a fine sand with a mean *t/d50* =231. Scour around the scAUR™ with VorGAUR™ model never occurs at the incipient open-bed scour speed for any of these sediments. This means that in a practical application the scAUR™ with VorGAUR™ foundation will not have any scour at flow speeds when there is open-bed scour of the same bed material. The approach flow speed for incipient scour around the foundation of the scAUR™ with VorGAUR™ model is at least 25% greater than the incipient open-bed scour speed for the same bed material.

Earlier, the scAUR™ and VorGAUR™ products were proven to prevent scour on vertical wall abutments. Here the performance of scAUR™ and VorGAUR™ concepts for more abutment designs was examined in model scale AUR flume tests. Spill-through and wing-wall abutment flume models, with and without scAUR™ and VorGAUR™ product features, were tested and show that scAUR™ and VorGAUR™ product features prevent scour around wing-wall abutments and for spill-through abutments, with only very minor scour downstream of a spill through abutment.

The effects of contraction scour, long-term degradation scour, settlement and differential settlement of footers, undermining of the concrete scAUR™ segments, and variable surrounding bed levels were examined. An additional curved ramp fairing surface (AUR Patent Pending) in the front of the scAUR™ fairing foundation prevents undermining of the foundation by open bed scour for piers and abutments and causes loose open-bed materials to be moved to the foundation sides. It was tested successfully in the AUR flume.

A full-scale scAUR™ and VorGAUR™ pier model was designed and constructed for testing in a large flume. Tests of the performance of full-scale scAUR™ and VorGAUR™ products on this model for 5 different configurations were conducted in the large flume at the Iowa Institute for Hydraulic Research during May 2013, with no scour around the model, after full-scale model flow blockage effects were considered, which were comparable to results for the 1/7 size models in the AUR flume. Manufacturing and installation processes for scAUR™ and VorGAUR™ products were refined, showing that stainless steel versions are the most cost effective for retrofitting piers and abutments and that steel scAUR™ concrete forms are the most cost effective for new construction bridge piers and abutments. Costs and plans are presented for the Route 360 bridge and the Route 613 bridge over the Dry River.

It should be noted that rip rap countermeasures are not acceptable design elements for new bridges (HEC 23, subsection 2.1.1; VDOT Drainage Manual, subsection 12.3.2). To avoid liability risk to engineers and bridge owners, new bridges must be over-designed to withstand 500-year superfloods, assuming that all sediment is removed from the 'scour prism' at that flow rate (HEC 23, 2.1.1). The scAUR™ products avoid liability risk by preventing or drastically diminishing the scour prism and reducing the cost of new bridge engineering and construction. Eliminating or drastically diminishing the scour prism greatly reduces the probability of failure, by the tenets of catastrophic risk theory.

Before this project, AUR performed a cost benefit analysis of scAUR™ with VorGAUR™ at that time as compared to current scour countermeasures *(8).* Published information shows that current expenses are required for scour monitoring, evaluation, and anti-scour mitigation design and construction, usually with rip-rap. For a bridge closed due to scour, the cost to motorists due to traffic detours is estimated to be as great as all other costs combined, but are not included in the analysis *(8)* and Figure ES.3 below. Even though the scour evaluation cost for single bridge is low, due to the large number of bridges in the US, the total cost for evaluation is large. The cost for scour evaluation takes more than 50% of public budgets allocated to scour.

The benefits of scAUR™ and VorGAUR™ to bridge owners and managers include actual large cost reductions over the life of a bridge by reducing the frequency and complexity of current monitoring practices for scAUR™ and VorGAUR™ fitted bridges and elimination of temporary repairs and countermeasures that require costly annual or periodic engineering studies and construction to mitigate scour on bridges at risk. Risks and liabilities due to a catastrophic failure are avoided with scAUR™ and VorGAUR™, whereas catastrophe theory shows a finite probability of failure with current temporary measures.

For an existing bridge, Figure ES.3 shows the present value ratio of the cost of current and future temporary countermeasures to the cost of installing pre-cast concrete scAUR™ products versus remaining bridge life with various times between inspections and repairs for an example bridge with six piers and two abutments requiring protection, using annual 7% inflation and 5% tax exempt interest rates to compute the present value of future expenses. **Even for bridges with little life left, current temporary countermeasures are much more expensive when the present value of future expenses is considered. Stainless steel scAUR™ and VorGAUR™ retrofits to existing bridges cost about half as much as precast concrete, so the ratio of the cost of current temporary countermeasures to the cost of stainless steel scAUR™ retrofits is at least double that shown in Figure ES.3.**

There is no situation where scAUR™ and VorGAUR™ products cost more than current countermeasures. There is no situation where any type of scour is worse with the use of the scAUR™ and VorGAUR™ products than without

them. The more frequent that scouring floods occur, the more cost effective are scAUR^{TM} and VorGAUR^{TM}. Clearly, scAUR^{TM} and VorGAUR^{TM} products are practical and cost-effective for US highway bridges.

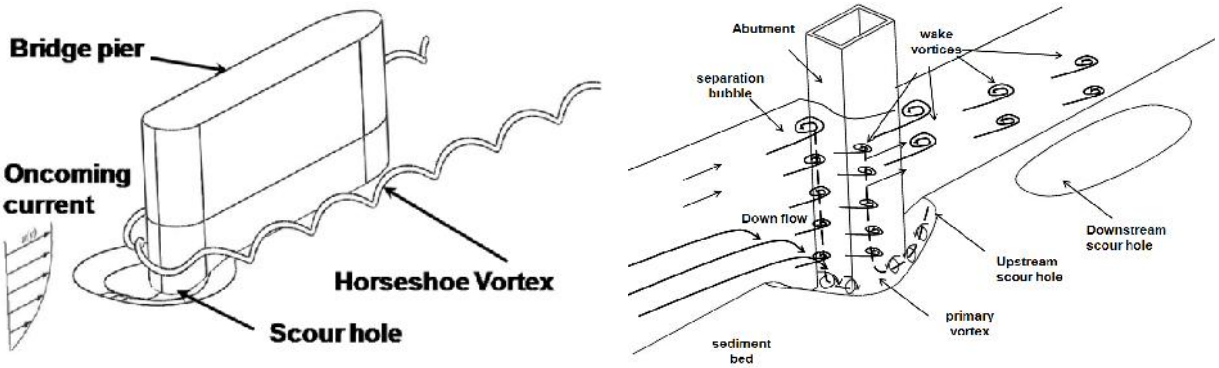

Figure ES1. (Left) The formation of a discrete horseshoe vortex at a bridge pier. (Right) Discrete shed vortex structures around a vertical wall abutment. Sketches from flow visualizations in AUR flume.

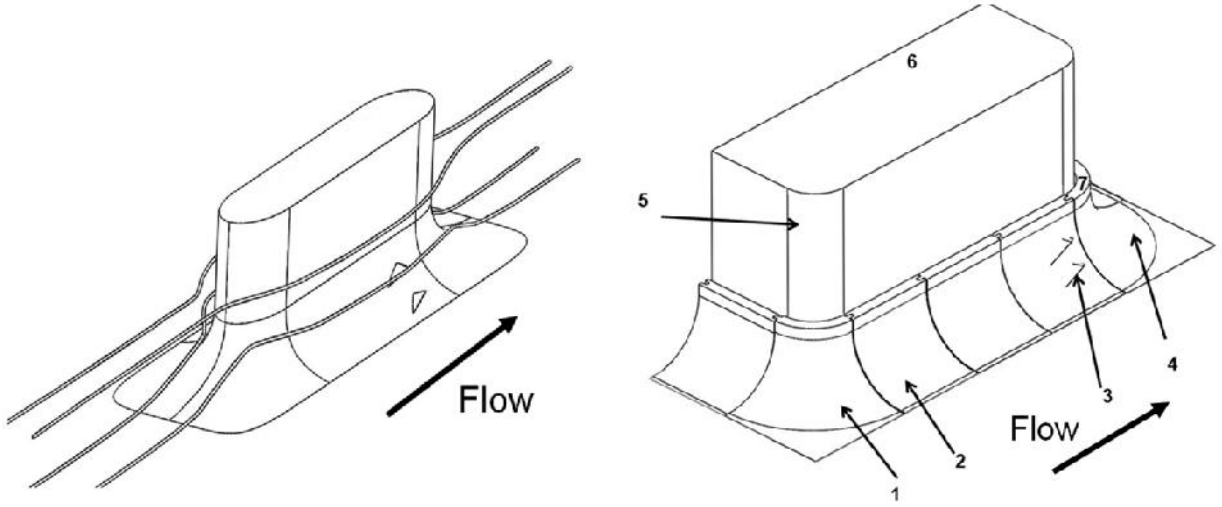

Figure ES.2. Left: (a) Flow streamline patterns around the scAUR^{TM} pier fairing with VorGAUR^{TM} vortex generators obtained via CFD simulation by AUR. Right: (b) an example abutment (6) scAUR^{TM} fairing (1,2,3,4,5) with VorGAUR^{TM} vortex generators (3).

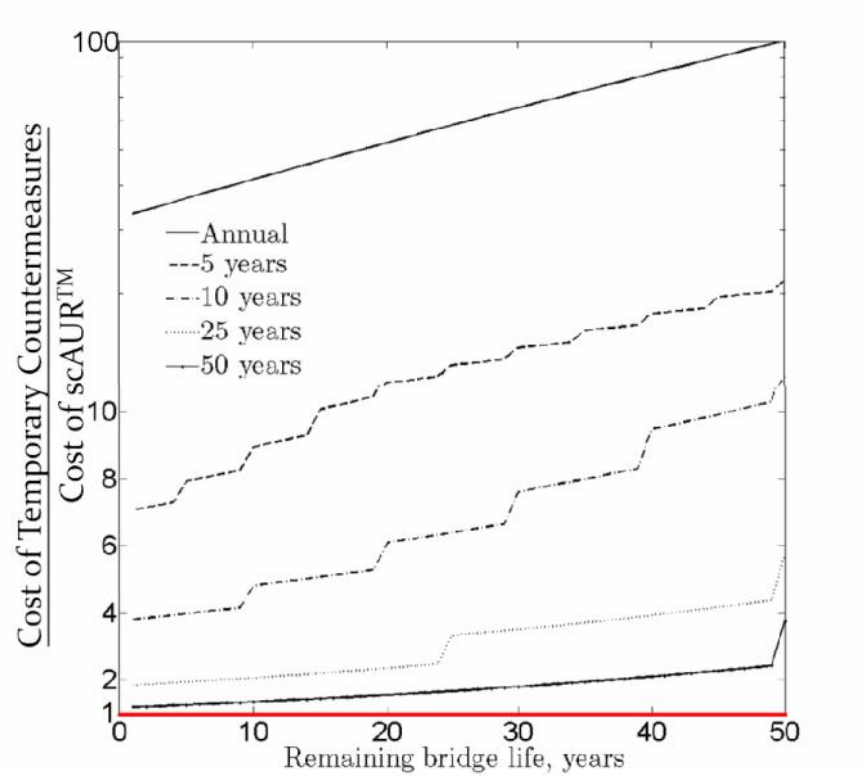

Figure ES.3 Ratio of the Present Value of all current and future temporary scour countermeasure expenses to the present value of pre-cast concrete scAUR™ with VorGAUR™ products.

IDEA PRODUCT:

Scour of bridge piers and abutments is one of the most common causes of highway bridge failures. All current countermeasures are temporary and do not prevent the main cause of local scour, which is large-scaled discrete vortices that form around underwater structures from flow separations. Using the knowledge of how to prevent the formation of these discrete vortices, prior to this NCHRP- IDEA project AUR developed, proved using model-scale tests, and patented new local-scouring-vortex-prevention products (scAUR™ as US Patent No. 8,348,553 and VorGAUR™ as US Patent No. 8,434,723) that are practical long-term permanent solutions to the bridge pier and abutment local scour problem, no matter what types and sizes of soil and rocks surround the pier or abutment.

In this project AUR provided computational and experimental evidence that the local-scouring-vortex-prevention products scAUR™ and VorGAUR™ prevent local scour at full scale for a variety of conditions and geometries. These products can be manufactured and installed cost effectively for retrofits to existing bridges and for new bridge construction, as planned by AUR.

CONCEPT AND INNOVATION:

The basic concepts of this innovation are (a) that the shape of the **scAUR™** streamlined fairing **prevents local scour** by preventing the formation of scouring vortices over and around the fairing and (b) the **VorGAUR™** vortex generators located well above the river bed **prevent separation and scour** on the downstream part of the fairing and cause some near river bed flow on the sides of the fairing to move up onto the fairing and **prevent scour of the side bed**. As proven by earlier AUR model flume tests, the scAUR™ streamlined pier or abutment fairing prevents the formation of scouring vortices and their highly fluctuating velocities and pressures and **prevents any scour** over a range of +/- 20 degrees angle of attack of the flow to the pier, decreases the near-surface flow speed, unsteadiness, and turbulent velocity and pressure fluctuations over the adjacent river bed next to the fairing base that **prevents scour**, increases the near-surface flow speed over the downstream fairing which reduces the river depth, reduces flow blockage of the pier or abutment as compared to a same projected frontal area scouring vortex case which reduces the river depth, reduces the overall pier or abutment drag, prevents the collection of debris because the streamlined flow without a horseshoe vortex deflects objects and debris away from the underwater structure**,** and protects the bottom of the pier from impact loads. **No previous bridge pier or abutment scour countermeasure**

uses aero/hydrodynamics to prevent scouring vortex formation and lift the upstream flow up and over the fairing. In contrast, a vertical nose pier or abutment always forms horseshoe vortices next to the river bed that scour even at low flow speeds that are below open bed incipient scour speeds (Figure ES.1, above). Furthermore, **scAUR™ with VorGAUR™ is much more cost effective** than current scour countermeasure costs.

Before this project, AUR performed a cost benefit analysis of scAUR™ with VorGAUR™ at that time as compared to current scour countermeasures *(8).* The benefits of scAUR™ and VorGAUR™ to bridge owners and managers include actual large cost reductions over the life of a bridge by reducing the frequency and complexity of current monitoring practices for scAUR™ and VorGAUR™ fitted bridges and elimination of temporary repairs and countermeasures that require costly annual or periodic engineering studies and construction to mitigate scour on bridges at risk. Risks and liabilities due to a catastrophic failure are avoided with scAUR™ and VorGAUR™, whereas catastrophe theory shows a finite probability of failure with current temporary measures.

INVESTIGATION:

The results for the several aspects of this project are summarized in separate sections below. **Section I** describes the selection of a candidate scour-critical bridge in Virginia for the manufacture and installation of full-scale scAUR™ and VorGAUR™ products on at least one pier and one abutment. While much work at model size has been done to prove these products, in **Section II** Reynolds number and bridge pier and abutment size effects were examined using computational fluid dynamics (CFD) in order to help prove the applicability of these products at full scale. In **Section III** data on the performance of these products with several smaller size sediments at model scale were obtained in the AUR flume in order to prove the applicability of the products for fine sediments. The performance of scAUR™ and VorGAUR™ concepts for a larger class of abutments was examined by model scale flume tests in **Section IV**. **Section V** shows the effect of a curved leading edge ramp for the foundation to counteract the effects of contraction scour, long term degradation scour, settlement and differential settlement of footers, undermining of the concrete scAUR™ segments, and effects of variable surrounding bed levels.

The full-scale scAUR™ and VorGAUR™ model that was developed for testing is described in **Section VI**. The results of full-scale tests of scAUR™ and VorGAUR™ products in a large flume facility are reported in **Section VII**. Simultaneously, manufacturing processes for scAUR™ and VorGAUR™ products were refined to provide multiple options for production and sizes, to reduce costs, to increase quality, and to expand applicability to more scour-critical bridges, as discussed in **Section VIII**. **Section IX** presents the plans and cost estimates for the manufacture of full-scale scAUR™ and VorGAUR™ products that were developed for at least one pier and one abutment of the selected scour-critical bridge in Virginia. All of these results prepares AUR to provide these scAUR™ and VorGAUR™ products to more state DOT customers, thereby making the commercial enterprise financially sustainable.

I . SELECTION OF A SCOUR- CRITICAL BRIDGE IN VIRGINIA FOR THE MANUFACTURE AND INSTALLATION OF FULL-SCALE SCAUR™ AND VORGAUR™ PRODUCTS

The next phase of developing the practical use of these innovations is to develop specific plans for the prototype manufacture and installation of full-scale scAUR™ and VorGAUR™ products on at least one pier and one abutment for a selected scour-critical bridge in Virginia that has a record of flooding and is representative of scour-critical bridges across America. Only the selection of a scour-critical bridge in Virginia is discussed here, while the manufacturing and installation processes are discussed in Sections VIII and IX below. The criteria required for candidate bridges were traffic volume, age, number of spans, and scour critical rating. The ideal candidate bridge would be a newer bridge with two piers, high average daily traffic, a scour rating of three or lower, and access to river flow data.

The Route 613 Bridge over the Dry River in Rockingham County, Virginia and the Route 638 bridge over the South River, Caroline County, Va were suggested as candidate bridges early in this project by VDOT personnel. Both were visited by AUR staff and are discussed in reference *(8).* There appears to be drawbacks to using either of these bridges in a full-scale demonstration project that is designed to prove the scAUR™ and VorGAUR™ products *(8).* The Route 613 bridge piers are at 45 degrees to the flow and will require additional features and costs for scAUR™ and VorGAUR™ products to prevent scour, as discussed more in Section IX. The Route 638 bridge has a low traffic volume and has deteriorated and may be replaced *(8).* AUR and VDOT personnel discussed installation ideas for the Route 613 Bridge in a conference call on Nov. 19, 2012. AUR continued to examine bridge information to help select the best candidate Virginia bridge for installation of scAUR™ and VorGAUR™ products.

Using the 2012 Virginia data from the National Bridge Inventory (NBI), three other candidate bridges for full-scale testing of the scAUR™ and VorGAUR™ products were found.

The primary candidate bridge is: "Bridge ID #: 1231; County: Amelia; Body of water: Appomattox River; Road: Route 360, Patrick Henry Highway (west bound); Year built: 1982; ADT: 8,995 vehicles per day; Spans: 3; Piers: 2; Scour rating: 3." The July 2008 Inspection Report (taken from uglybridges.com) indicates that for channel protection, "Bank is beginning to slump. River control devices and embankment protection have widespread minor damage. There is minor stream bed movement evident. Debris is restricting the channel slightly.[level 6]". For scour protection, the "**Bridge is scour critical; bridge foundations determined to be unstable.** [level 3]."

This bridge meets all of the desired criteria and appears to be an ideal candidate for a full scale test. The Appomattox River that runs under the bridge is a substantial waterway and would likely provide more consistent flow conditions for testing than a creek or dry river. This bridge also has the advantage of being over 20 years newer than the other bridges, which means it is earlier in its design life and not scheduled to be replaced. Based on the inspection report, it appears that the two piers have very similar flow exposure and sediment erosion. It is reasonable to assume that with the piers behaving similarly in the past and with a straight flow direction, that these piers will experience similar scour conditions. Even though the footing is only exposed on pier 2, both have had scour problems and sediment erosion. The scour problem does not appear to be as severe or advanced as the Route 613 bridge, but it has more consistent flow conditions. The inspection report also has a recommendation to place "rip rap in eroded areas under structure and along exposed Pier 2 footing". The scAUR™ retrofit could be placed instead of rip rap and provide a good full-scale test. The width of the piers is not mentioned, but based on the diagrams, photos, and a visit by AUR staff, they appear to be about two feet in width. The abutments are only up near the bridge deck on the sloping bank and are currently covered with 1' – 2' rip rap.

A secondary candidate bridge is: "Bridge ID #: 18130; County: Stafford; Body of water: Aquia Creek; Road: Route 310, Garrisonville Road; Location: 2.4M RTE644-0.3M RTE643; Year built: 1957; ADT: 9,442 vehicles per day; Spans: 4; Piers: 3; Scour rating: 3." The Nov. 2009 Inspection Report (taken from uglybridges.com) indicates that for channel protection "Bank protection is being eroded. River control devices and/or embankment have major damage. Trees and brush restrict channel. [level 5]." For scour protection, the "**Bridge is scour critical; bridge foundation determined to be unstable.** [level 3]."

This bridge is not as ideal as the Appomattox River bridge, but it appears to have some good features for testing the scAUR™ retrofit. The three piers have similar sediment levels and scour issues for a comparative test. Based on the aerial diagram, the majority of flow is between piers two and three, but the creek bed is flat enough that all of the piers would experience flow during a flood. This bridge is old and in need of other repairs, but has piers that appear to be one to two feet wide. For some reason, scour protection is not listed under the recommended repairs/additions in the 2012 Inspection report. Even so, the report does state that there is scour. None of the pier footers are exposed, which means that the condition is not as severe as the Route 613 bridge. Additionally, the scour does not appear to be occurring at a high rate since the sediment level around the piers has not changed drastically from when it was measured in 1999 and 2007.

A tertiary candidate bridge is: "Bridge ID #:18018; County: Spotsylvania; Body of water: Massapanox Creek; Road: Leavells Road; Location: 0.7M RTE208-1.9M RTE628; Year built: 1956; ADT: 8,869 vehicles per day; Spans: 3; Piers: 2 (not verified); Scour rating: 3." The Sept. 2009 Inspection Report (taken from uglybridges.com) indicates for channel protection "Bank is beginning to slump. River control devices and embankment protection have widespread minor damage. There is minor stream bed movement evident. Debris is restricting the channel slightly. [level; 6]." For scour protection, the "**Bridge is scour critical; foundation determined to be unstable**. [level 3]."

This bridge is a less than ideal candidate for a full scale test. Unlike the Appomattox River Bridge, this bridge does not span a substantial waterway and is relatively old. It has issues other than scour and appears to need substantial renovation or replacement work. Scour seems to be only an issue for pier two, and the flow conditions are very different for the two piers. Based on the profile and aerial diagrams, only pier two is below the normal water level. In addition, the height of the piers is less than ideal. Pier one is buried and has less than five feet of clearance under the bridge, based on the side view picture. There appears to be more clearance around pier two, but not much room to maneuver. One positive aspect is that the bed level seems to fluctuate regularly and the scour is progressing at a decent rate. Regardless, this bridge appears to be even less ideal than the one on Route 613. The 2012 inspection report recommends installation of scour countermeasures, but it appears that it will not be a good place to test the scAUR™ with VorGAUR™ products.

During this proposed demonstration project, AUR should have access to information to document the flow level history of the waterway that is selected for installation of the scAUR™ and VorGAUR™ products. For this purpose a professional hydrologist who is associated with AUR performed an assessment of the data that are and will be

available for these 5 bridges *(8)*. The goal of the assessment was to determine which of the five candidate bridges has the greatest potential for accurate stream stage and/or discharge estimation and, consequently, is most ideal for a fair hydrologic assessment of bridge scour conditions before and after installation of the scAUR^{TM} products. The assessment criteria were (1) availability of streamflow data from USGS river gauges at or near each bridge and (2) the type(s) of available data and duration of data record.

The Appomattox River has two operational instantaneous discharge gauges: one upstream and another downstream of the Patrick Henry Highway bridge. Short of having a gauge at the bridge itself, this is the most ideal arrangement: flood volumes can be very well constrained by having upstream and downstream discharge measurements. The period of record for the upstream gauge (USGS 02040000 Appomattox River at Mattoax, Va.) is the longest of all the gauges, and as a result the most accurate flood frequency estimates can be made for this gauge.

Considering the type and duration of streamflow data available near the five candidate bridges, the westbound Patrick Henry Highway bridge over the Appomattox River is the most attractive option for a scAUR^{TM} and VorGAUR^{TM} retrofit installation demonstration project. Based on the other selection criteria discussed above, it is also the best candidate since it is a relatively new bridge and has at least two piers, a high average daily traffic, and a scour-critical rating of three or lower.

II – COMPUTATIONAL FLUID DYNAMICS RESULTS FOR A FULL-SCALE PIER COMPARED WITH LOW REYNOLDS NUMBER MODEL-SCALE RESULTS

While much computational and experimental work at model size has been done by AUR to prove these products, Reynolds number and bridge pier size effects were examined using computations in order to help prove the applicability of these products at full scale. Since the V2F Reynolds-averaged Navier-Stokes (RANS) model in the Open Foam code has been proven to accurately compute 3D flows and the presence of any separation or discrete vortices (*3*,*4*,*8*,*9*,*10*), then the behavior of mean streamlines, the local surface pressure coefficient ($C_p = 2\ (P - P_e)/\rho U_e^2$), and the local surface skin friction coefficient ($C_f = 2\ \tau/\rho U_e^2$) are sufficient to determine if any separation or discrete vortices are present. Some results are presented below and are compared with the low Reynolds number case previously computed by AUR on its computer cluster in 2008; more results are in reference *(8)*. Table II.1 gives lists of parameters for the 2 Reynolds number cases. Note that to avoid CFD grid work and unnecessary expense, the high and low Reynolds number cases used the same grid, but achieved a high Reynolds number with changes in flow speed and kinematic viscosity. The non-dimensional results do not depend on speed or properties since all non-dimensional results are presented in terms of non-dimensional parameters.

For the low Reynolds number case, Figure II.1 shows a perspective view from downstream of near-wall streamlines that pass through X/t = 7.24 at Y/t = 0.013, where X is the stream-wise position measured from the beginning of the straight side of the pier, Y is the vertical position measured from the open bed surface, and t is the pier width. No vortices or separation are observed upstream of the stern or tail of the model. Figure II.2 is a description of the higher Reynolds number case. There are similar features for the high Reynolds number case, which are shown in Figure II.3. Figures II.4 show comparisons of the C_p for the low and high Reynolds number cases at the same Y/t locations. An important feature in these plots is the lack of any abrupt changes in the slope of C_p over a short distance, which means that there is no discrete vortex formation and separation. Figures II.5 show comparisons of the C_f for the low and high Reynolds number cases. One does not see any abrupt changes in the slope of C_f , also an indicator of no separation or discrete vortex formation. The non-dimensional drag ($\text{drag}/(\rho U_e^2/2)(\text{surface area})$) on the pier is clearly lower for the higher Reynolds number case than the lower Reynolds number because C_f is always lower at higher Reynolds numbers and the overall drag is an integral of ($C_f\ \rho U_e^2)/2$ over the pier surface. In addition, these results show that the smooth flow over the pier produces lower drag force or flow resistance and lower flow blockage than a pier without the scAUR^{TM} shape because low velocity swirling high blockage vortices are absent. As a result, water moves around a pier or abutment faster above the river bed, producing a lower water level at the bridge and lower over-topping frequencies on bridges during flood conditions for any water level when no discrete vortices are present.

There are no discrete vortices or separation on the nose and side regions of the scAUR^{TM} shape for either Reynolds number. The VorGAUR^{TM} vortex generators that are used in practice on the sides of the scAUR^{TM} shape prevent separation on the tail or stern of the scAUR^{TM}. Vortex generators are widely proven and used in aero/hydrodynamic practice at model and full scale to prevent separation over stern or tail regions. Thus, from the CFD results full-scale models will work as well at preventing scouring vortices as at model scale.

Differences between model-scale and full-scale experimental scour results have also been addressed by previous work. From the Wilson Bridge Study (http://www.fhwa.dot.gov/publications/publicroads/00marapr/hydra.cfm):

"Two different methods were used for extrapolating model results to full scale. One was a geometric scaling procedure, which is the traditional technique of scaling the scour hole in proportion to the length ratios used to model the structure. The other is a University of Florida procedure proposed by Dr. Sheppard; this procedure uses the ratio of the structure width to sediment size as a scaling parameter. Dr. Sheppard has demonstrated that this parameter explains a lot of the discrepancies between measured field data and scour predictions from equations based on geometric scaling of laboratory data. Interestingly, the 3-D numerical model results agreed quite well with the results of the physical model with Dr. Sheppard's scaling parameter. The design team was intrigued by this procedure but opted not to use it because it yielded significantly lower scour estimates, thus less conservatism, for a very important structure."

Recently published research sponsored by the National Co-operative Highway Research Program (NCHRP) using hundreds of sets of scour data by Sheppard et al. *(5)* shows that model scale bridge scour experiments produce much more severe scour depth to pier size ratios than the scour depth to pier size ratios observed for full-scale cases due to scale effects. "The data from the larger-structure laboratory tests clearly show a decreasing dependence of equilibrium scour depth on the structure size as the structure size increases. The physics of why this occurs remains unproven. Some attempts have been made to explain this phenomenon, e.g., Ettema et al. *(6)* and Sheppard et al. *(7).* Ettema et al. investigated the differences in the scale of the turbulence in the wake region with increasing pier size and associated this with the decreasing dependence of scour on increasing pier width. Sheppard gave a theoretical explanation involving the pressure-gradient field surrounding the structure. According to the hypothesis, pressure gradients in the vicinity of the structure due to the presence of the structure are much larger for the smaller structures than for larger ones. The forces on the sediment grains produced by the pressure gradients are larger near small structures than for larger prototype structures. This explains why predictive equations based on small-scale laboratory data over predict scour depths at prototype-scale structures. Stated another way, for a given sediment size, some local scour mechanisms diminish in magnitude with increasing structure size." **More discussion given in that report supports the conclusion that scour predictive equations, developed largely from laboratory data, over predict scour on full-scale underwater structures.**

Based on the past work and experience of AUR *(2,3,4),* more physical evidence and insights support the idea that scour preventing devices will work better at full scale than model scale. Scouring forces on river bed materials are produced by pressure gradients and turbulent shearing stresses, which are instantaneously unsteady. As shown in Figure II.4, at higher Reynolds numbers the non-dimensional pressure gradients are lower, which supports Sheppard's hypothesis. Also, as shown in Figure II.5, at higher Reynolds numbers the surface skin friction coefficient is lower than at lower Reynolds numbers, so less scour occurs at higher Reynolds. **Thus, the scAUR™ and VorGAUR™ will work just as well or better in preventing the scouring vortices and any scour at full scale as at the proven small model scale.** Other CFD by AUR that is not reported here, shows that scAUR™ and VorGAUR™ products prevent scouring vortices around bridge piers downstream of bending rivers *(8).*

	Low Re	High Re
Ue, m/s	27.4	4.6
scAUR™ pier width(t), m	0.076	0.624
δ, m	0.039	1.71
Θ, m	0.003	0.133
Re_t	$1.34x10^5$	$2.19x10^6$
Re_δ	$6.82x10^4$	$6.02x10^6$
Re_θ	$5.36x10^3$	$4.73x10^5$
ν, m^2/s	(air)$1.56x10^{-5}$	(water) $1.31x10^{-6}$

Table II.1 List of flow conditions for the low and high Reynolds number CFD cases. Low Reynolds number case was completed prior to the current NCHRP -162 project.

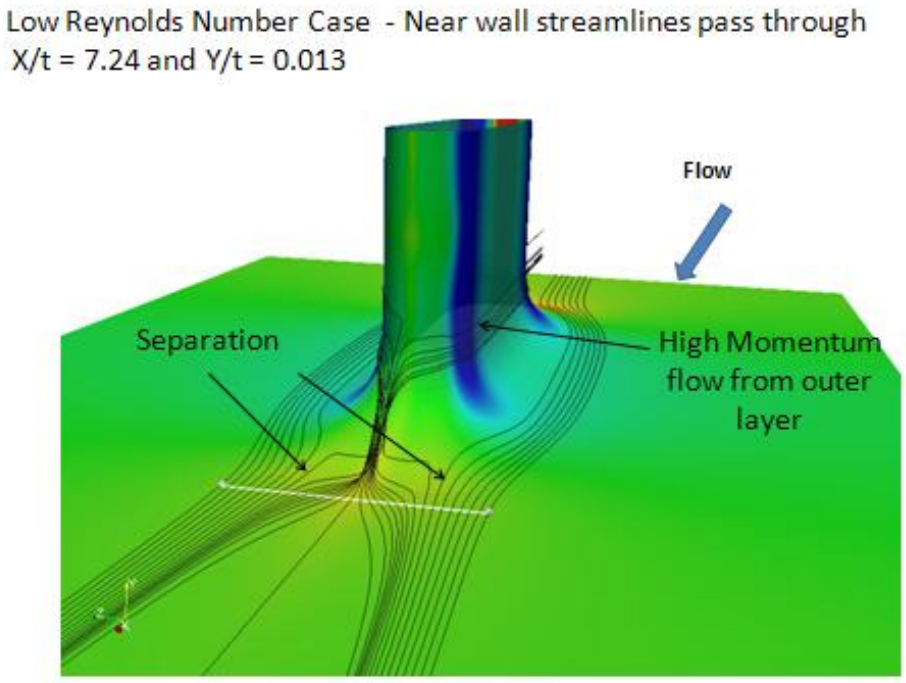

Figure II.1 Downstream view of the low Reynolds number case. The flow streamlines indicate no discrete vortex formation on nose and sides.

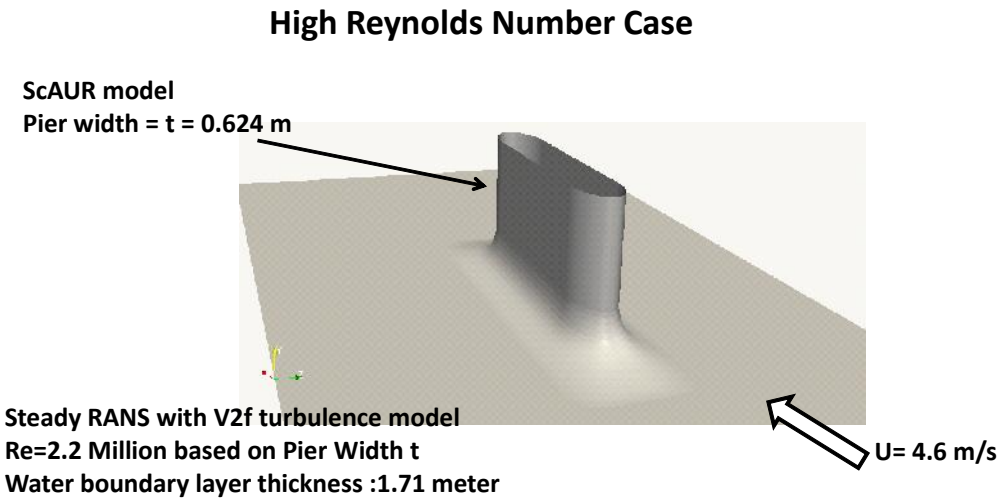

Figure II.2 Description of high Reynolds number CFD case. Right-handed co-ordinate system: X = 0 at the upstream location of the straight pier side; Y = 0 at bottom of fairing; Z = 0 at centerline of pier.

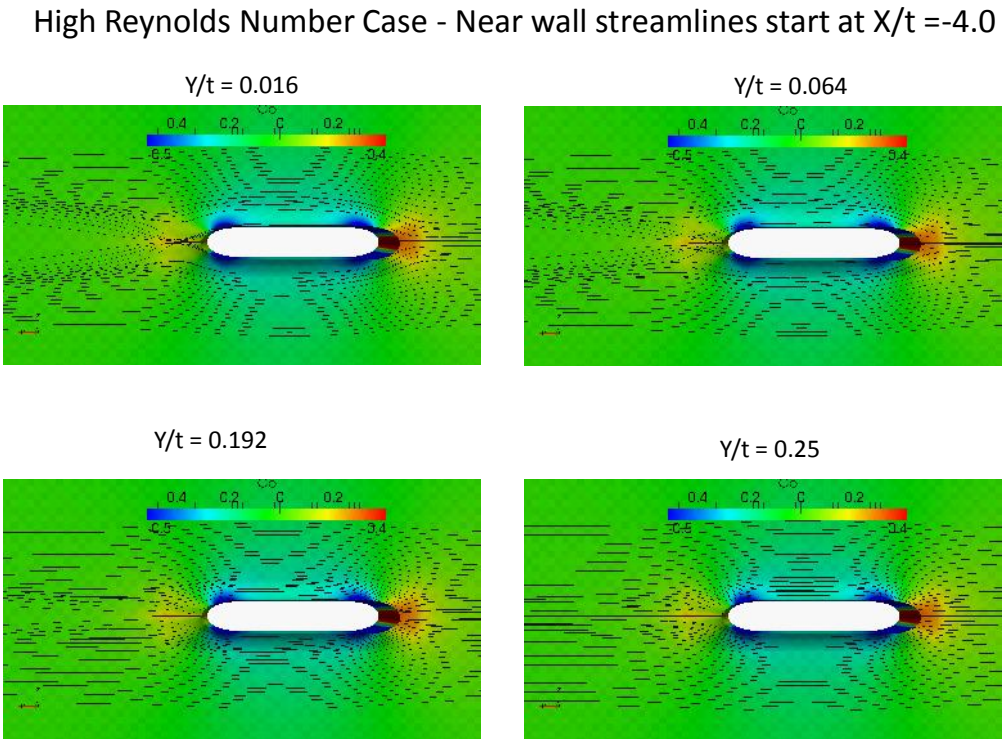

Figure II.3 High Reynolds number case. Streamlines near the wall show no formation of discrete vortices and separation over the front nose of the scAUR™.

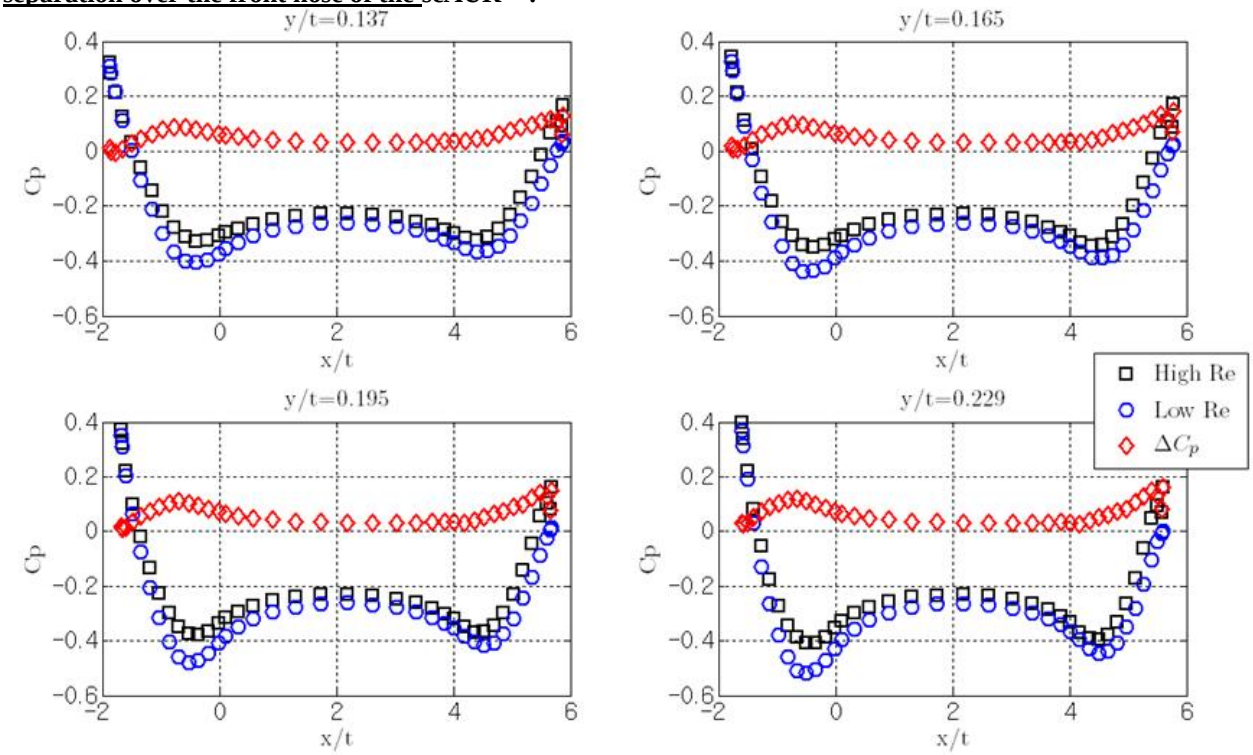

Figure II.4 Local surface pressure coefficient ($C_p = 2 (P - P_e)/\rho U_e^2$) at various Y/t versus X/t for both Reynolds numbers.

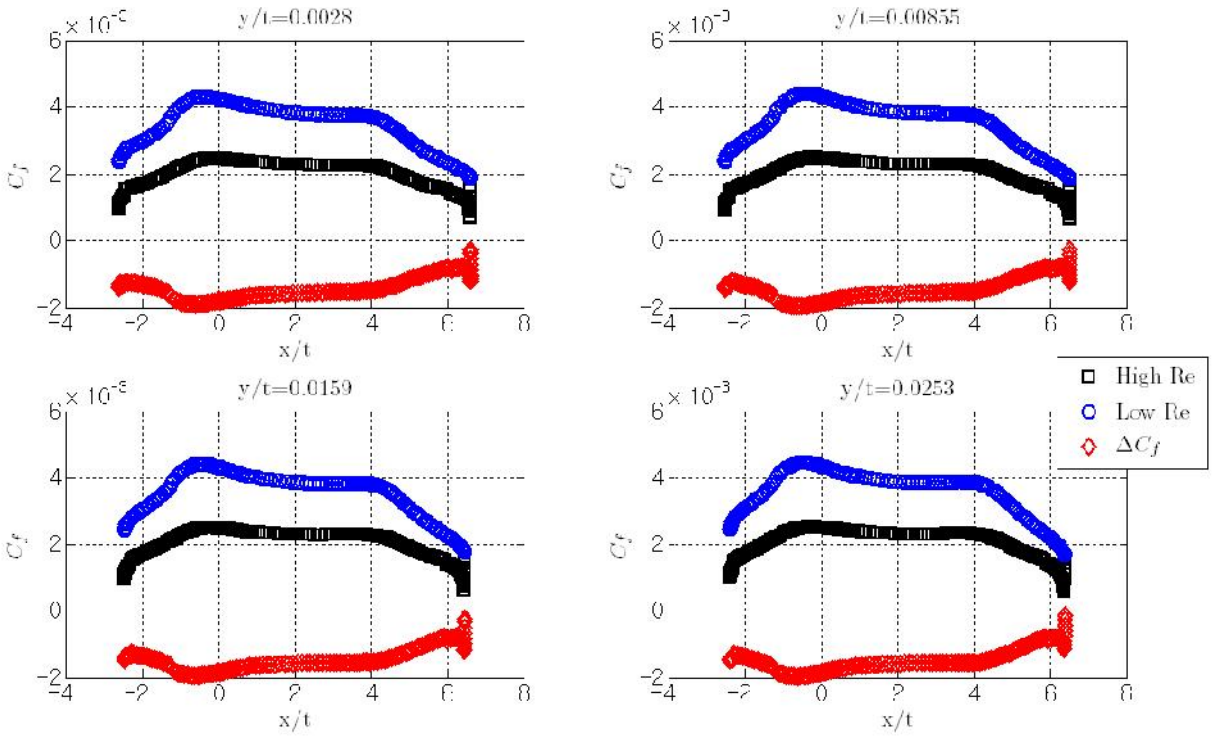

Figure II.5 Local surface shear stress (skin friction) coefficient ($C_f = 2\ \tau/\rho U_e^2$) at various Y/t versus X/t for both Reynolds numbers. High Reynolds number black symbols; low Reynolds number blue symbols; difference between high and low Reynolds number in red.

III FLUME TESTS WITH SEVERAL SMALLER SIZE SEDIMENTS AT MODEL SCALE

Since all earlier model flume studies had used a single-size-range of pea gravel (specific gravity = 3.0) of 1/8" to ¼" (3.2mm to 6.4mm), data on the scour-preventing performance of these scAUR™ and VorGAUR™ products with several smaller size sediments at model scale were obtained in the AUR flume to prove the applicability of the products for finer sediments *(8).* AUR used published open literature information by Melville *(11*) on the greatest scouring conditions for a circular cylinder case in selecting sediment sizes *(8*). From Melville the greatest equilibrium scour depth occurs around a circular pier (width = t) when it is surrounded by uniform sediment at times when the flow velocity equals the critical value (i.e. incipient conditions for open bed scour, which fall in the "clear water" range). Also, live bed scour depth is never larger than incipient scour depth. Melville states: "Recent data by *Sheppard et al.* (*7*) demonstrate **significant scour depth reductions for increasing *t/d50* when *t/d50* > 50**. ***Thus, local scour depths at field scale may be significantly reduced from those observed in the laboratory."*** The "*t/d50*" term is the ratio of pier width to median grain diameter. **AUR used a value of *t/d50*=50, with data over a range of sediments from 38.1 to 64.6**.

Three sieved black slag (specific gravity = 3.7) gravel sizes were used to encompass this range of previously reported conditions where scour will be the greatest for the AUR t = 76.2mm wide circular cylinder pier model. Gravel in this size range are difficult to obtain. Only a small amount of each size was available after sieving a large amount of raw material. The sizes are **Gravel A**: 1.18 to 1.4 mm (64.4 > *t/d50* > 54.4); **Gravel B:** 1.4 to 1.7mm (54.4 > *t/d50* > 44.8); and **Gravel C**: 1.7 to 2mm (44.8 > *t/d50* > 38.1). No distribution of the gravel size within each range was determined.

A goal of this work is to examine scour around the scAUR™ with VorGAUR™ fairing under flow conditions when there is incipient open bed scour. Usually smaller sediment scours at a lower flow speed than larger pea gravel because the weight of a particle holding it in place varies with its volume, whereas the flow forces acting to dislodge the particle vary with the area of the particle (*6,11*). Using a higher flow speed when incipient open bed scour occurs for a larger particle will be a stronger test of the scAUR™ with VorGAUR™ model surrounded by black slag, so the pea gravel was used in the open bed away from the pier model for these cases, as shown in Figure III.1.

Figure III.1. Photo of AUR 4 foot (1.22m) wide flume test section looking downstream with black gravel around the scAUR^{TM} model (middle of photo), the comparison circular cylinder (right of photo), and pea gravel away from the model. The 1/8" to ¼" (3.18mm to 6.35mm) pea gravel produces open bed scour at higher water speeds than the open bed scour of the black gravel. Note the location of the pitot-static probe 1m upstream of the scAUR^{TM} with VorGAUR^{TM} model.

Tests were made in the AUR flume facility. As shown in Figure III.1, the centerline of the 29" (0.737m) long and 9" (0.229m) wide pier, fairing, and foundation scAUR^{TM} with VorGAUR^{TM} model was parallel to and 20" (0.51m) from a flume side wall near the stream-wise middle of the flume gravel box. The 3" (76.2mm) wide pier is 18.12" (0.460m) long. A given black slag covered 5" (127mm) on each side and downstream of the model and 7" (178mm) in front. In order to have familiar comparison scour test cases for these sediments, a vertical 3" (76.2mm) diameter circular cylinder was located 7.5" (191mm) from the other side wall at the stream-wise location of the downstream end of the pier of the scAUR^{TM} with VorGAUR^{TM} model, as also shown in Figure III.1. The same black sediment for a given case was located around the cylinder with the area of 3" (76.2mm) in front, 2" (50.8mm) on each side, 1.5" (38.1mm) in the rear and 3" (76.2mm) deep before the test**.**

The flow velocity across the flume width in front of the model is uniform within 3%. The free-surface bow wave generated by the pier model did not influence the surface flow that approached the circular cylinder. Using a string on the end of a handheld-wire inserted into the flow, the flow patterns around the pier and cylinder models were examined. The flow patterns around each model appeared to be symmetric.

The experiments for the 3 sizes of black slag gravel were run at a nominal speed (Uref) of 0.64±0.03 m/s close to the free surface when incipient open bed scour of the pea gravel was observed. The front and back curved fairing height for the AUR model is about 0.0762 m. The water free surface height is about 2.17 times of the pier fairing height or 6.5" (0.165m) and simulates a typical condition of river flow around a bridge pier. At a reference location of about 1 m upstream of the pier model and upstream of the gravel box, the vertical smooth-wall mean velocity boundary-layer profile for the inflow was taken with a Prandtl-type pitot-static pressure probe (*8*), shown in Figure III.1, and measured with a U-tube manometer. This boundary-layer-velocity profile shown in Figure III.2 follows the law-of-the-wall profile near the flume bottom and the law-of-the-wake profile near the free surface (*8,9*). The boundary layer thickness "delta" is about 0.125 m at 99.5% of free-surface velocity. The Reynolds number based on the momentum thickness is about 12000.

Scour occurred around the circular cylinder model for gravel A, B and C at water speeds much lower than speeds when incipient open bed pea gravel scour started (*8*). For the cylinder pier model, the scour hole was generated at the model nose and a deposition mound is formed downstream as the result of the scour, which is a typical result (*11*).

The flume tests at the speed when incipient open bed scour of the pea gravel occurred were conducted until no more scour around the circular cylinder was observed, which was less than one hour. The gravel bed level around the scAUR^{TM} with VorGAUR^{TM} model was measured by a laser-based optical method (*12*) before and after each test (*8*). The gravel bed level around the cylinder pier model was also measured after the test. **No scour was observed around the scAUR^{TM} with VorGAUR^{TM} model for any black gravel size at speeds when the open bed pea gravel began to scour** (*8*), within the y/t = +/- 0.004 measurement uncertainty, as shown Figure III.3 for gravel A. In Figure III.3, the few pea gravel shown on the black gravel were carried by open bed scour from upstream. No mound of black gravel is generated and only a few black gravel were carried farther downstream of the model.

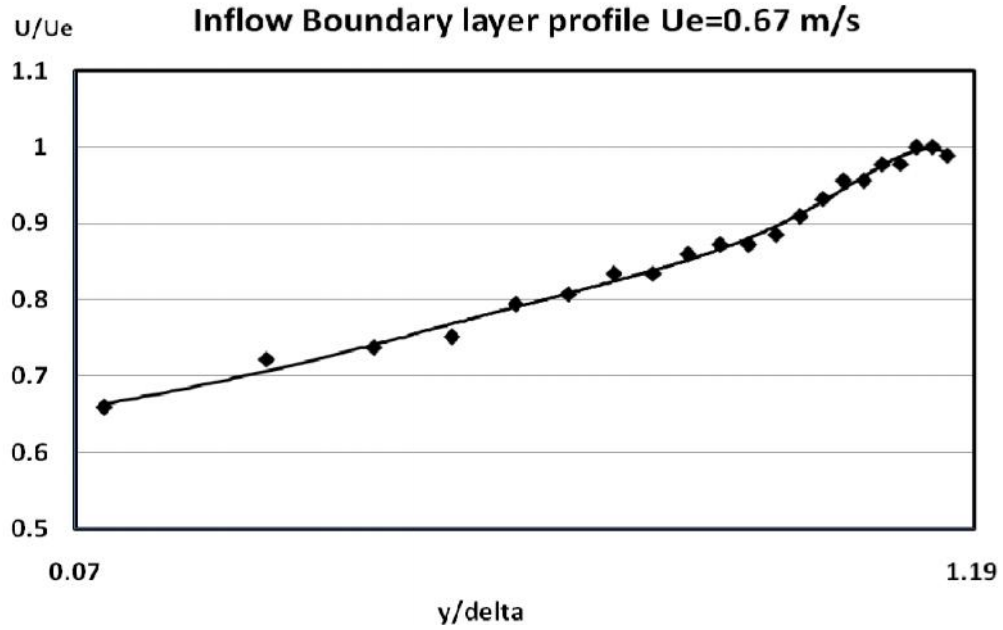

Figure III.2. Flume test section inflow centerline mean velocity profile. Wall friction velocity Utau = 0.028m/s.

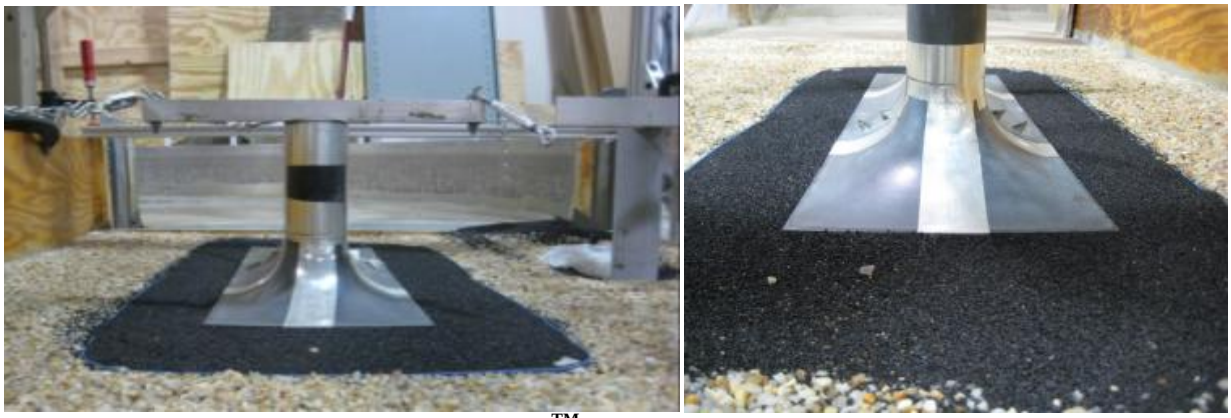

Figure III.3. Black slag gravel A around scAUR^{TM} model showing no scour after a test. View from upstream (left); view from downstream (right).

Tests were also conducted at higher flume speeds for gravel B black slag to determine the speed and locations where scour occurred around the scAUR^{TM} with VorGAUR^{TM} model. As discussed above, no scour occurred around the model at an incipient open bed pea gravel scour speed of 0.64±0.03 m/s. To increase the flow speed and examine the black slag scour around the scAUR^{TM} with VorGAUR^{TM} model, 0.011" (0.28mm) thick sheet metal plates were used to cover the pea gravel upstream and around the scAUR^{TM} with VorGAUR^{TM} model, that are shown in Figure III.1 without the sheet metal plates, in order to prevent the open bed pea gravel scour. Scour at the upstream end of the black slag in front of the scAUR^{TM} with VorGAUR^{TM} model, which is just downstream of the sheet metal

covering the pea gravel, began at 0.8 m/s, but there was no scour around the model. Since this smooth sheet metal floor boundary layer has a higher near-flume-floor surface speed than that for any rough upstream floor for the same water free-open-surface speed, the incipient scour speed around the scAUR^{TM} with VorGAUR^{TM} model would be an even higher speed.

Flume tests also were performed with a fine sand, which is the finest sediment examined. This screen-sieved sand had a size distribution by weight of: 0.5% greater than 0.047" (1.19mm), 3.7% between 0.047" (1.19mm) and 0.024" (0.61mm), 58.5% between 0.024" (0.61mm) and 0.0098" (0.25mm), and 37.3% smaller than 0.0098" (0.25mm). The average size by weight is about 0.013" (0.33mm), which is $t/d50$ = 231. The sand is distributed around the scAUR^{TM} with VorGAUR^{TM} model like for the black slag and a portion was located in the open bed. At a free-stream speed of 0.4m/s there was incipient open-bed scour of the sand. There was no scour observed around the model at this speed.

Several general observations and conclusions can be made from earlier AUR flume tests and the current experiments. Clear water scour around a circular cylinder will occur even at low speeds for all of the tested sediments. Scour around the scAUR^{TM} with VorGAUR^{TM} model never occurs at the incipient open-bed scour speed for any of these sediments. This means that in a practical application the scAUR^{TM} with VorGAUR^{TM} foundation will not have any scour at flow speeds when there is open-bed scour of the same bed material. The approach flow speed for incipient scour around the foundation of the scAUR^{TM} with VorGAUR^{TM} model is at least 25% greater than the incipient open-bed scour speed for the same bed material.

IV – FLUME TESTS OF scAUR^{TM} AND VorGAUR^{TM} CONCEPTS FOR A LARGER CLASS OF ABUTMENTS

Earlier before this project, the scAUR^{TM} and VorGAUR^{TM} products were proven to prevent scour on square-corner vertical wall abutments at free-stream flow speeds when there was incipient open-bed scour (*8 and www.noscour.com*). Here the performance of scAUR^{TM} and VorGAUR^{TM} concepts for a larger class of abutments is examined in model scale AUR flume tests. Spill-through and wing-wall abutment flume models, with and without the scAUR^{TM} with VorGAUR^{TM} scour-prevention product features, were tested in order to examine the level of improvements.

Flume tests of a wing-wall abutment without scAUR^{TM} and VorGAUR^{TM}

The wing-wall abutment flume model without scAUR^{TM} and VorGAUR^{TM} products is shown in Figure IV.1. This test was done under the same conditions as the earlier square vertical wall abutment that was 10" (0.254m) high and L = 6" (0.152m) wide. Like the earlier abutment tests, a false wall was installed which reduces the flume width from 48" (1.22m) to 39" (0.99m), as shown in Figure IV.1. The 10" (0.254m) high L = 6" (152.4mm) abutment model with 45^{o} wings was attached to this false wall. The pea gravel (specific gravity of 3) and the size of 3.2-6.4mm were distributed on the flume bed as shown in Figure IV.1. Like the earlier square abutment, the flow area contraction ratio was 1.18 due to the presence of the abutment model. Like all earlier abutment tests, the water depth was 6" (0.152m). The near-free-surface flow speed is faster closer to the abutment, as given by values of 0.63m/s, 0.61m/s, 0.59 m/s, and 0.56 m/s at locations 1, 2, 3, and 4, respectively, in Figure IV.1. At this condition, there was incipient open-bed scour at location 1.

The flume was run for 45 minutes until the scour around the abutment reached equilibrium. Figure IV.2 shows the free-surface water level difference before and after the contraction leading edge. The flow accelerated in front of the contraction of the upstream wing and separated downstream of the contraction leading edge forming the free-surface vortex, as also shown in Figure IV.2. Flow visualization using a mobile yarn tuft on a wand also confirmed that the flow separated passing the leading edge of the contraction.

The local scour occurred around the contraction leading edge of the wing-wall abutment model and the maximum local scour depth is located very close to the contraction edge as shown in Figures IV.3 and IV.4. Figure IV.4 shows the scour depth contours normalized by the model length (L = 6" or 152mm). The maximum scour hole depth and mound height are approximately -0.13L and 0.12L, respectively. Both the earlier tested square vertical abutment (*8*) and the current abutment model with 45^{o} wings show very similar contraction leading edge scour patterns with the wing wall abutment having about a half of the scour depth of the square vertical wall at the contraction leading edge. The wing-wall abutment produces a more shallow free-surface vortex scour hole over a greater area downstream of the model as compared to the square vertical wall abutment.

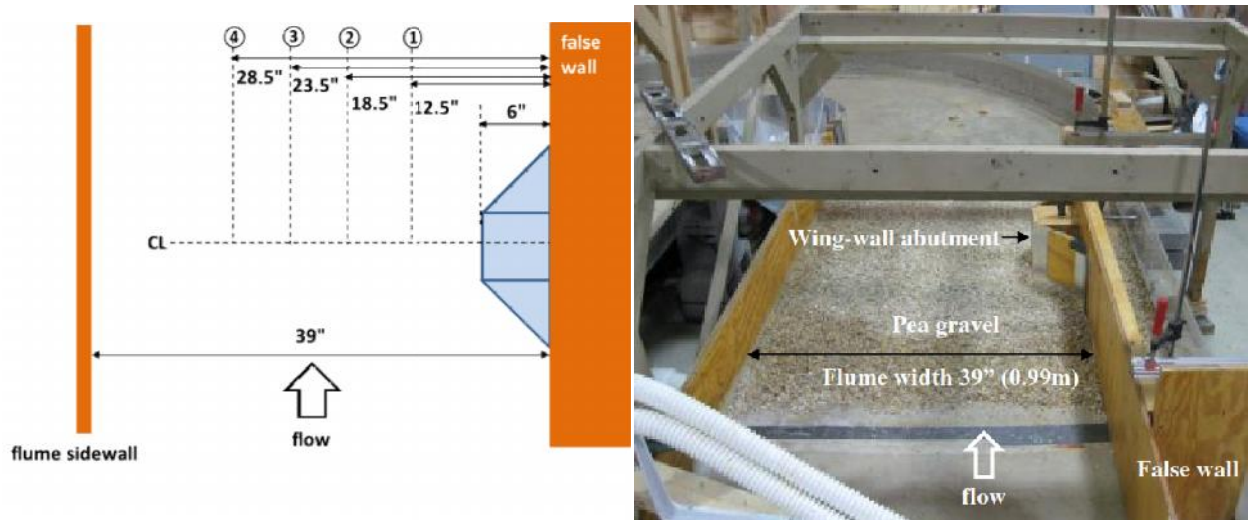

Figure IV.1. Wing wall abutment model without scAUR™ and VorGAUR™ products before test. Pea gravel of 3.2-6.4mm in size.

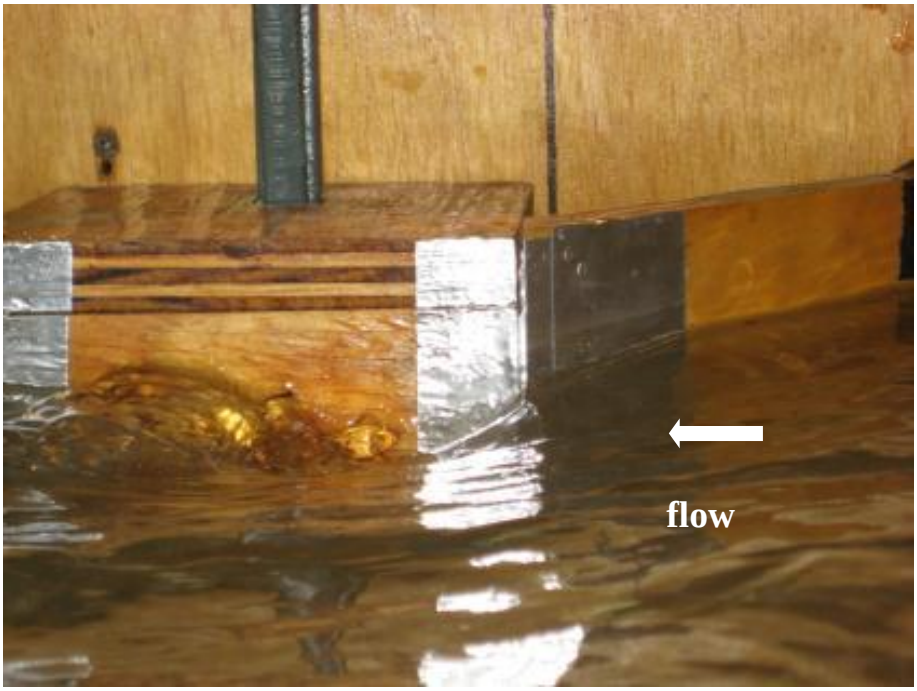

Figure IV.2. Closeup view of wing-wall abutment model. Note that free surface height change after the leading edge of the contraction due to separation.

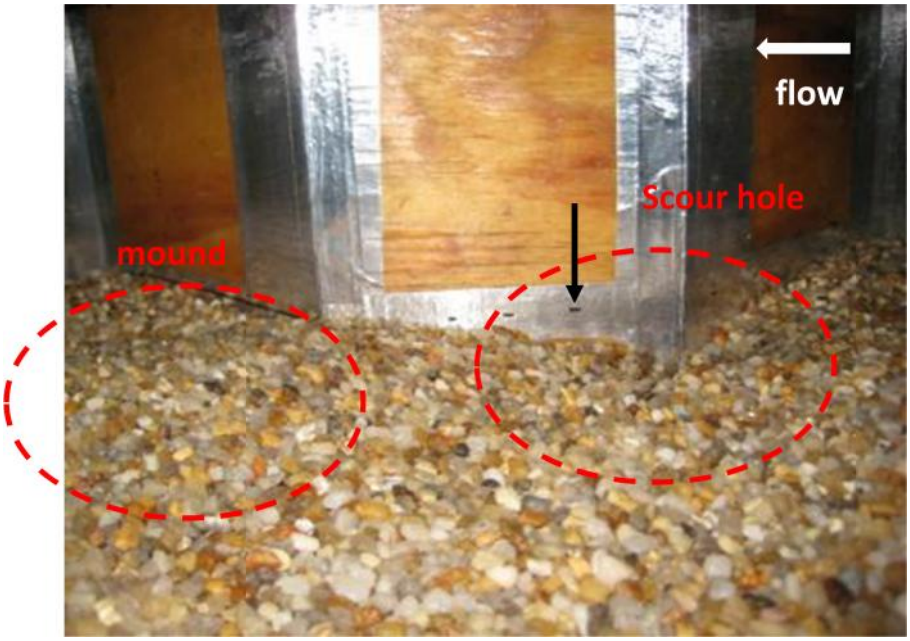

Figure IV.3. Scour hole and mound after test. Dashed line on model indicates the pea gravel level before the test.

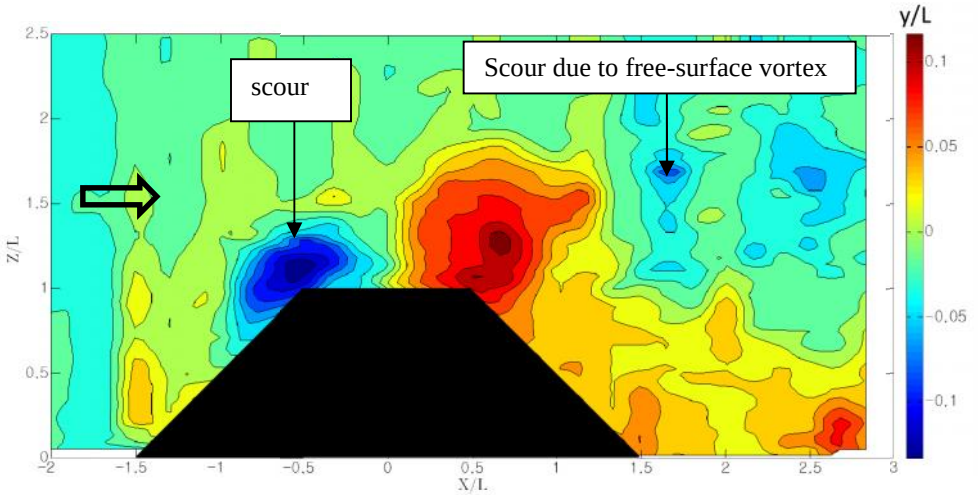

Figure IV.4. Bed level change contours after and before incipient open-bed scour flow around the wing-wall abutment model with length L into the flow <u>without</u> scAUR™ and VorGAUR™ products *(8)*. Flow from left to right.

<u>Flume tests of the wing-wall abutment with scAUR™ and VorGAUR™</u>

The same wing-wall abutment flume model that was tested above was modified with scAUR™ and VorGAUR™ products, as shown in Figure IV.5. A test was performed under the same flow conditions and flume geometry as for the wing–wall abutment without scAUR™ and VorGAUR™ products that is discussed above.

Figure IV.6 shows surface skin friction direction oilflow mixture results. It consists of a mixture of yellow artist oil paint and mineral oil that has low enough viscosity to flow with the skin friction lines. Yellow streaks are first painted about perpendicular to the flow direction on a black painted surface. The flow causes some oil to be carried downstream in a local flow direction, which can be observed against the black painted surface. Figure IV.6 clearly shows that the effects of the scAUR™ and VorGAUR™ products are to bring lower velocity flow up from the flume bottom and prevent the scour around the bottom of the abutment.

Figure IV.7 shows the free-surface water flow around the scAUR^{TM} with VorGAUR^{TM} abutment model. The flow accelerates around the contraction and separates downstream of the contraction. The tuft visualization also confirmed that the flow separated passing the contraction. The free-surface vortex still exists and a water level difference is clearly shown before and after the contraction edge in spite of the application of VGs.

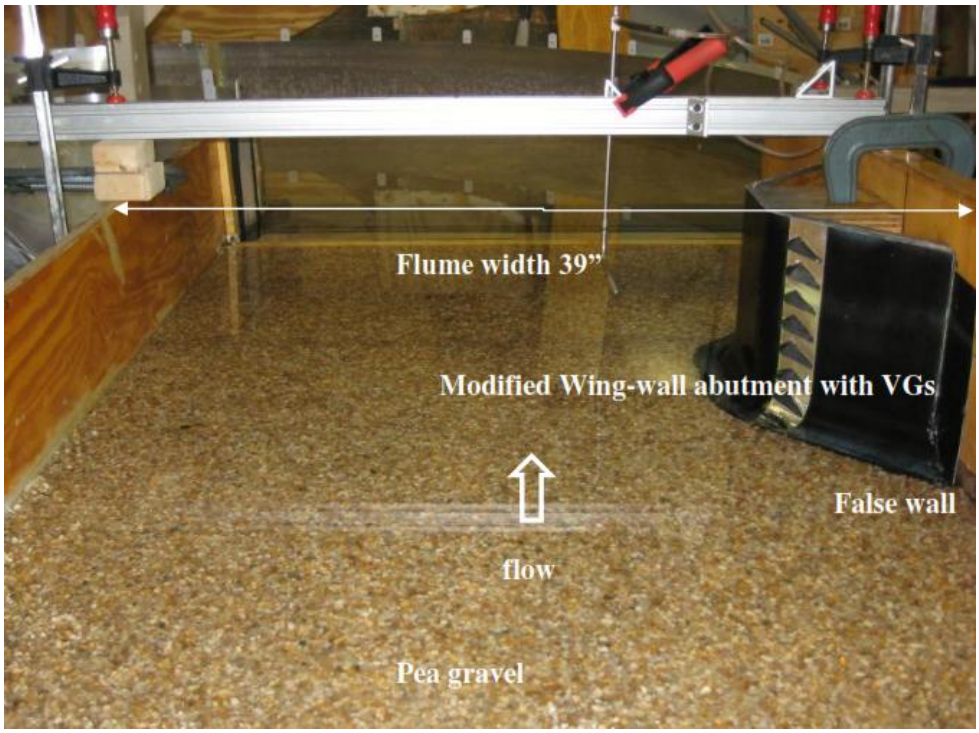

Figure IV.5. scAUR^{TM} with VorGAUR^{TM} modified wing wall abutment model with vortex generators (VGs) before the test. Pea gravel of 3.2-6.4mm in size.

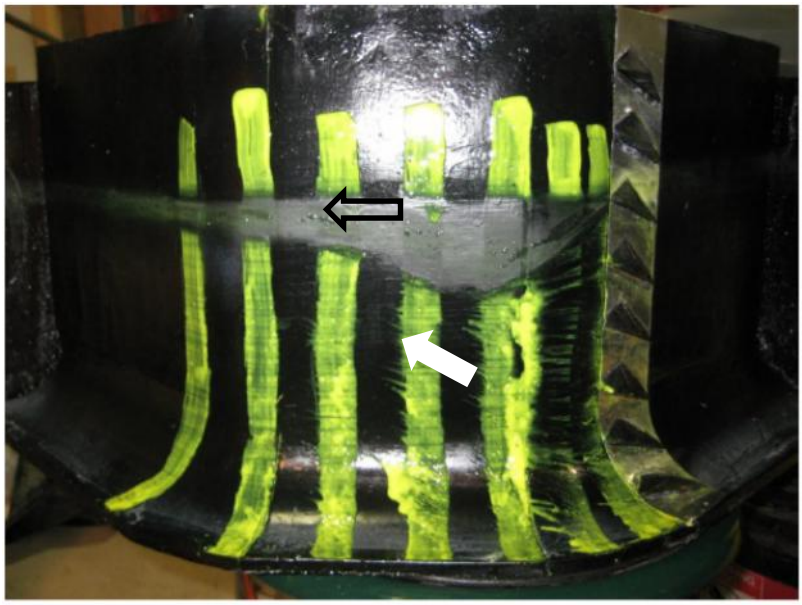

Figure IV.6. Surface oilflow results for the modified wing-wall abutment model with VGs. Flow is from right to left. The upward streaks show that the scAUR^{TM} and VorGAUR^{TM} products cause the flow to move up the wing-wall abutment. The gray region is produced by a mixture of the oilflow material and waterborne substances at the free surface.

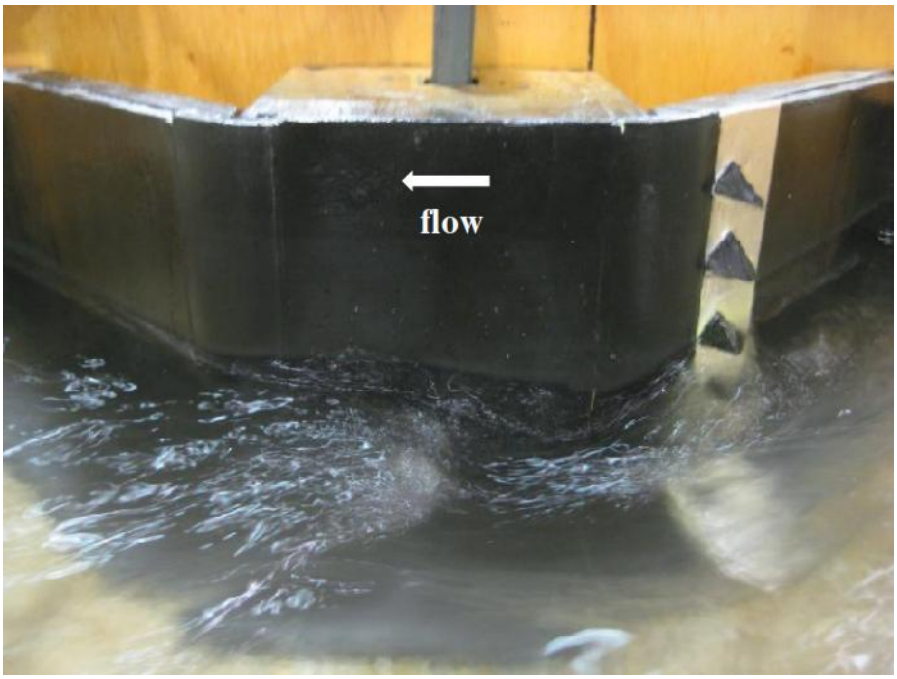

Figure IV.7. Close up view of the modified wing-wall abutment model with VGs. Note the free surface height change after the contraction due to the surface vortex.

With a scAUR^{TM} modified wing-wall abutment without VGs, there is no scour around the contraction and near the base of the modified wing-wall due to the fairing, but there is still some open bed scour downstream around x/L =2, like in Figure IV.4 due to the free-surface vortex. With the addition of VorGAUR^{TM} VGs, there is not only no scour around the model base, but there is no open bed scour hole farther downstream of the model around x/L = 2, as shown in Figure IV.8. This is the effect of VGs on the surface vortex which caused the scour hole farther downstream of the unmodified model in Figure IV.4. The VGs generate the counter-rotating vortices which diffuse and reduce the strength of the surface vortex. **Thus, no scour occurred around the contraction and near the base of the modified wing-wall abutment with VGs and there is no scour farther downstream of the model.**

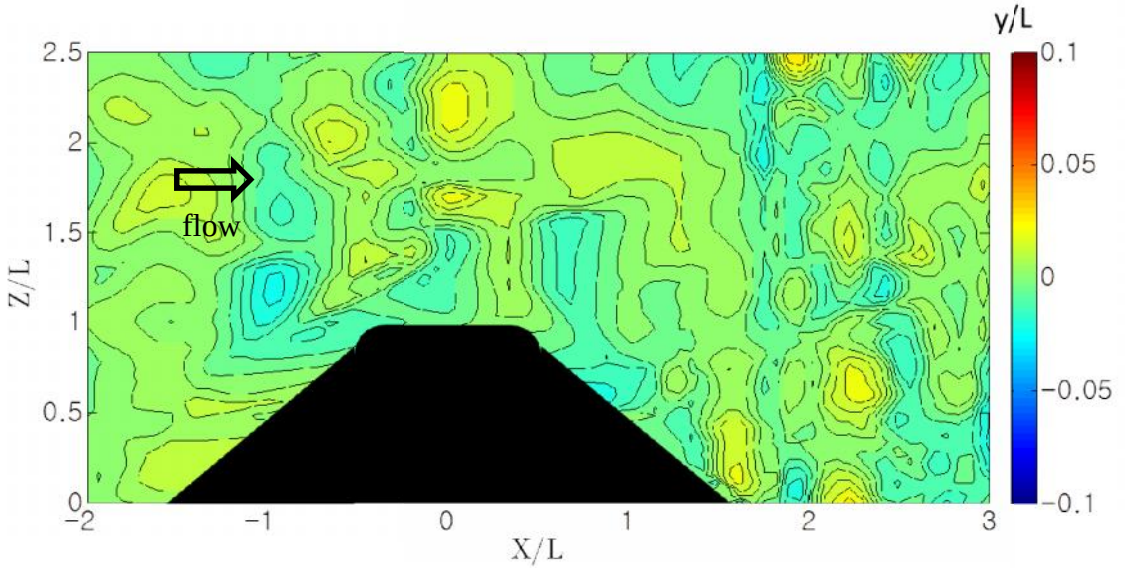

Figure IV.8. Bed level contours around the modified wing wall abutment model with VGs (length L=6.25”). No scour observed at any location.

Flume tests of a spill-through abutment without scAUR™ and VorGAUR™

The spill-through abutment flume model without scAUR™ and VorGAUR™ products is shown in Figure IV.9. It has a 45° slope and was tested under the same conditions as the wing-wall abutment above. The flow area contraction ratio was 1.10 due to the presence of the abutment model for a water depth of 5.5" (0.140m). The near-free-surface flow speed is faster closer to the abutment, as given by values of 0.63m/s, 0.61m/s, 0.59 m/s, and 0.56 m/s at locations 1, 2, 3, and 4, respectively, in Figure IV.9. At this condition, there was incipient open-bed scour at location 1.

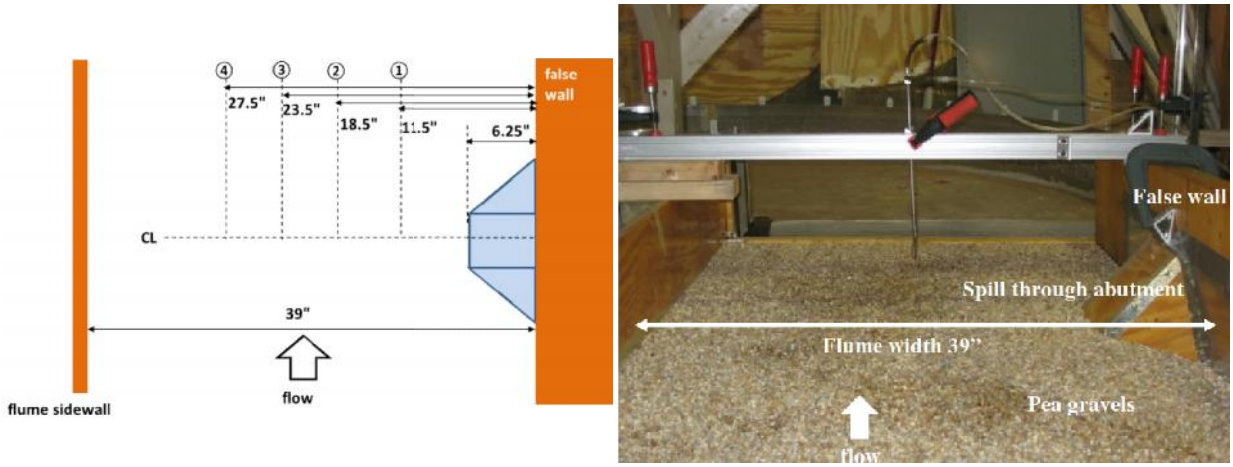

Figure IV.9. Spill through abutment model before test. Pea gravel of 3.2-6.4mm in size.

The flume was run for 45 minutes. Figure IV.10 shows a top view of the water flow around the abutment model in the flume. The flow accelerated around the contraction and separated downstream of the contraction leading edge as shown in Figure IV.10. Flow visualization using a mobile tuft on a wand also confirmed that the flow separated passing the leading edge of the contraction. The tuft seemed to fluctuate less than in the wing-wall abutment test, indicating a weaker separated flow. There was a free surface level difference before and after the contraction leading edge due to the free surface vortex formation. The local scour close to the model is very weak while a large scour hole was generated downstream of the model (x/L = 1.25-2.5 and z/L = 1) as shown in Figure IV.11. It is apparently caused by a stronger surface vortex shed from the model or closer to the bed than by the wing wall abutment. Figure IV.12 shows the scour depth contours normalized by the model length (L = 6.25"). The maximum scour hole depth is approximately -0.17L.

In a comparison of the bed level contours from the results of the wing-wall abutment (Figure IV.4) and the vertical wall square abutment (*8*), the spill-though abutment has the weakest scour near the model, but it has the scour hole at the downstream of the model with the similar order of depth of the vertical square corner wall due to the free surface vortex generated at the leading edge of the contraction.

Flume tests of a spill-through abutment with scAUR™ and VorGAUR™

The spill-through abutment flume model with scAUR™ and VorGAUR™ products is shown in Figure IV.13 and IV.14. The flume was run for an hour under the same flow conditions and flume geometry as for the spill-through abutment without scAUR™ with VorGAUR™ designs that is discussed above (*1).* The VorGAUR™ vortex generators are 2" (50.8mm) long by 0.5" (12.7mm) high. Figure IV.14 is a surface oilflow for this case that clearly shows that the scAUR™ and VorGAUR™ products bring lower velocity flow up from the flume bottom. The VGs diffuse the surface vortex by creating counter-rotating vortices and prevent the downstream scour around the bottom of the abutment. Figure IV.12 shows the deep scour hole for the untreated abutment. Without the VGs, there would still be some scour downstream. With a scAUR™ modified wing-wall abutment with VGs, Figure IV.15 shows no scour around the upstream contraction and near the base of the modified spill-through abutment due to the fairing. Although there is still a very minor scour at the downstream of the model, its max depth (-0.02L) is about the size of one pea gravel and is much lower than that for an untreated abutment.. **No scour occurred around the contraction and near the base of the modified wing wall with VGs. The open bed scour due to the free surface vortex has been prevented by the vortex generators**.

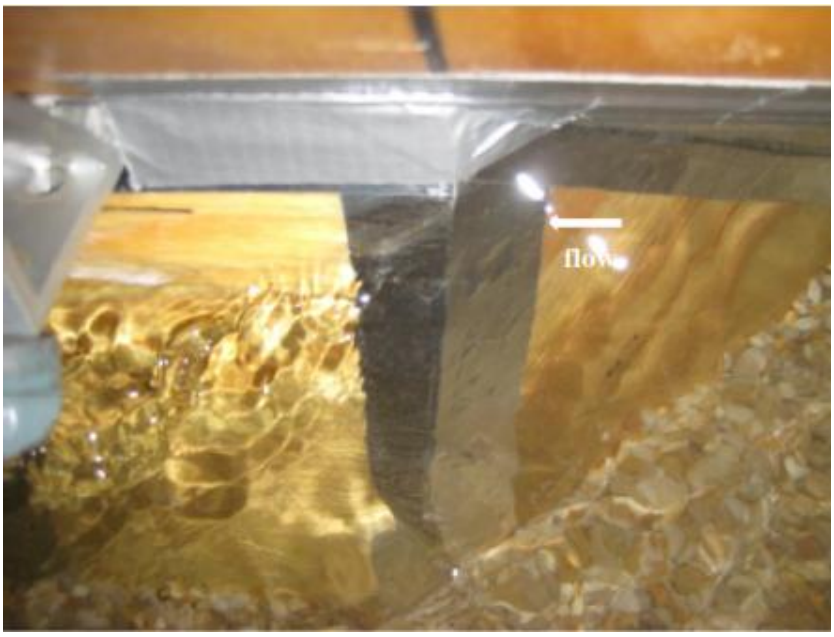

Figure IV.10. Top view of spill-through abutment. Flow is from right to left. Separated flow is clearly shown downstream of the leading edge of the contraction by the variations of refracted light on the free surface.

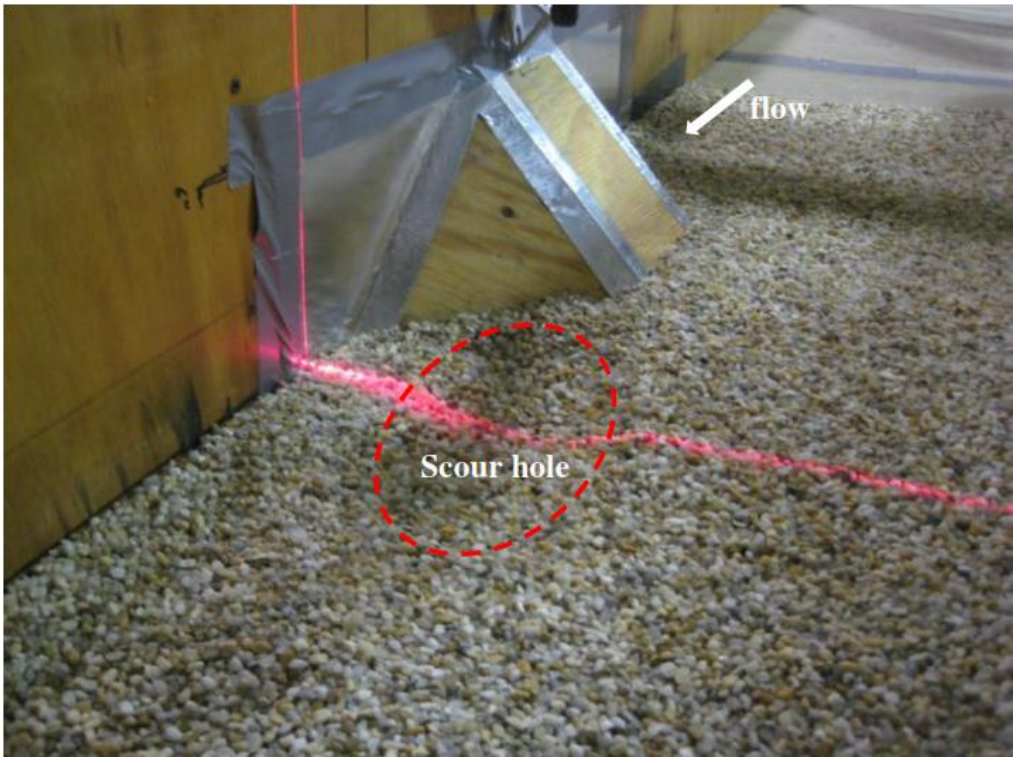

Figure IV.11. View from downstream. Scour hole was generated downstream of the model. Note the laser light sheet on the gravel showing the scour hole.

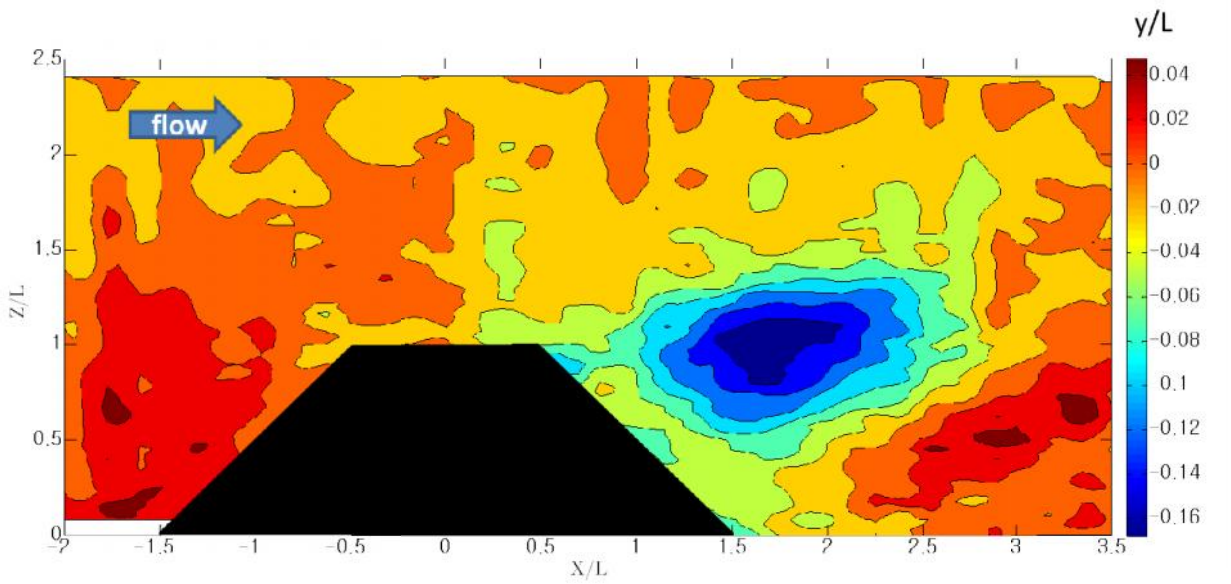

Figure IV.12. Bed level change contours after and before flow around the untreated spill-through model (L=6.25", 159mm). Note the dark blue scour hole.

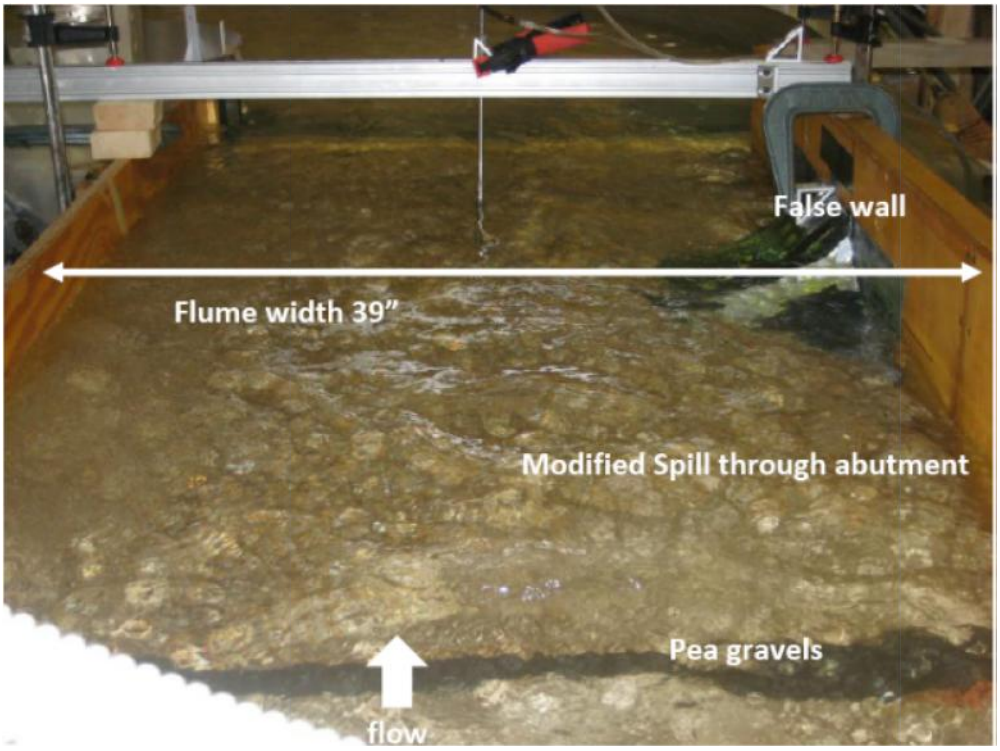

Figure IV.13. Modified sharp-edge spill-through abutment model with VGs in the AUR flume. Pea gravel of 3.2 to 6.4mm in size.

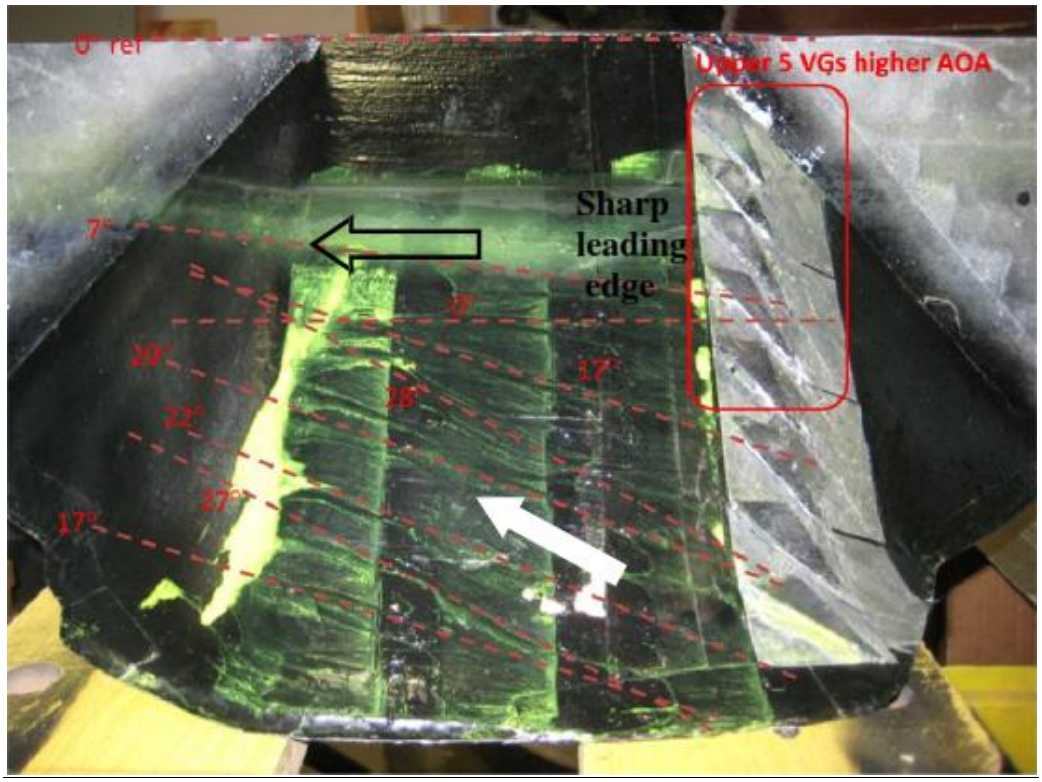

Figure IV.14. Surface oilflow results for modified sharp edge spill through abutment model with 8 VGs. Upper 5 VGs at higher angles of attack (AOA) than the lower VGs. Note that the scAUR™ and VorGAUR™ products cause the flow to move up the abutment as it moves downstream, bringing low speed fluid from the bottom of the river and preventing scour. The gray region is produced by a mixture of the oilflow material and waterborne substances at the free surface *(8)*.

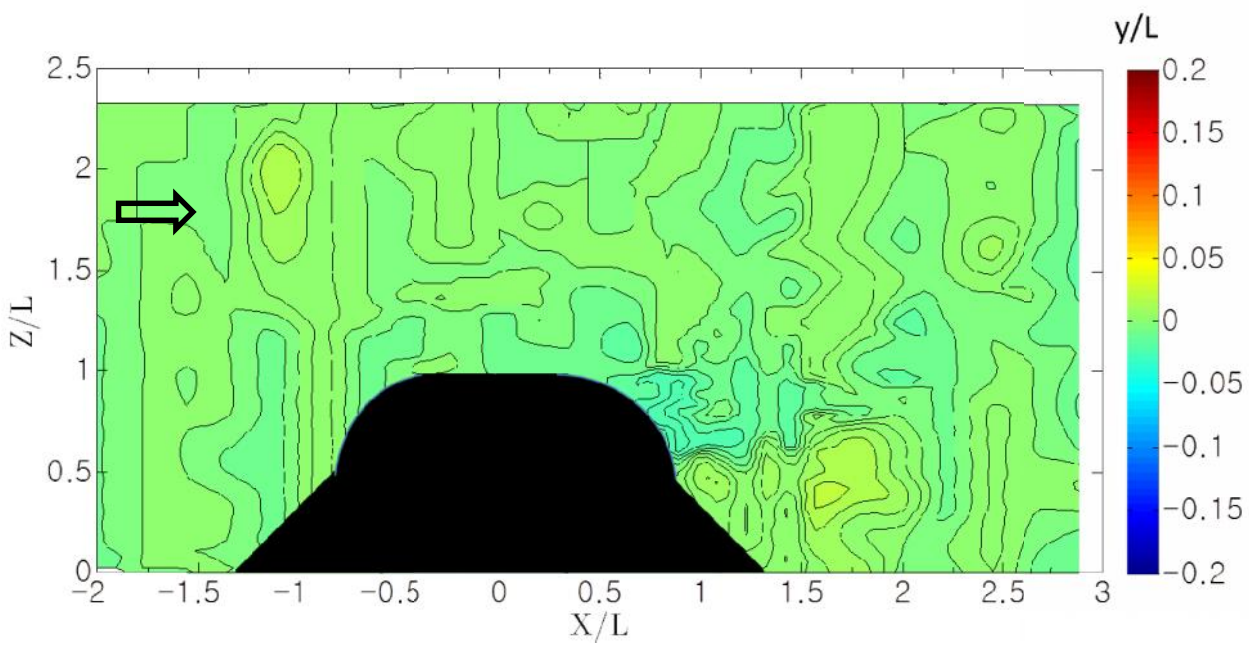

Figure IV.15. Bed level change contours after and before flow around the scAUR™ modified sharp edge spill through model with 8 VorGAUR™ VGs (L=9", 229mm).

V – TESTING OF PROTECTION FOR FOUNDATIONS EXPOSED BY OPEN-BED SCOUR

Aspects of the scAUR^{TM} and VorGAUR^{TM} design features have been expanded for use around the foundation (AUR Patent Pending) in order to further protect the foundation from the effects of contraction scour, long term degradation scour, settlement and differential settlement of footers, undermining of the concrete scAUR^{TM} segments, and effects of variable surrounding bed levels. This effort addresses issues that may undermine the foundation for the scAUR^{TM} and VorGAUR^{TM} products.

First, when the scAUR^{TM} and VorGAUR^{TM} design features are installed on a bridge pier or abutment, the scAUR^{TM} fairing prevents any scouring horseshoe vortex formation and downflow of higher velocity water from upstream and the VorGAUR^{TM} vortex generators cause low speed water flow near the river bottom next to the pier or abutment to move up the pier or abutment, as shown in Figures IV.6 and IV.14 above. Thus, the velocities, shearing stresses on the bottom of the pier or abutment, and pressure gradients will be lower than without the scAUR^{TM} and VorGAUR^{TM}. Presumably the surrounding river bed will be at the same height or level as the top edge of the scAUR^{TM} fairing at the bottom of the pier or abutment after installation. As all AUR flume studies have shown, under these conditions scour of the open bed material occurs at a lower river speed before scour of the material around the base of the scAUR^{TM} fairing occurs.

What this means is that scour of the river bed away from the scAUR^{TM} protected pier or abutment will occur first and that the river bed level will be lower away from the pier or abutment. If a pier or abutment foundation is exposed, it will still have a higher immediate surrounding river bed level than farther away. Even so, we would like to further arrest scour around the foundation to prevent high speed open bed scour from encroaching on the river bed material next to the foundation.

Second, if the front of the foundation of a pier or abutment is exposed to approach flows, then a foundation horseshoe or scouring vortex is formed at the front which will cause local scour around the pier or abutment. What this suggests is that we mount a curved ramp in front of the foundation that prevents the formation of this foundation horseshoe vortex. Additional pieces around the sides of the foundation are also another thought, but since they do not produce a flow that moves up the scAUR^{TM} fairing, they will not produce any benefit.

Based on these facts, flume tests were conducted with 3 foundation leading edge ramp configurations: (1) an exposed rectangular foundation with no front ramp protection, (2) an upstream curved-top trapezoidal planform foundation ramp with the side edges tapered toward the pier to produce a stream-wise vortex on each side to bring open bed materials toward the foundation, and (3) a curved-top upstream foundation ramp with a rectangular planform and straight spanwise edges that are parallel to the pier side, also to produce a stream-wise vortex on each side to bring open bed materials toward the foundation.

Flume tests for scour depth were made for these cases with a 0.5" (12.7mm) high foundation elevation (Figure V.1) with gravel A around the foundation with or without a leading edge ramp *(8)*. Gravel A was used since it was the smallest black gravel tested and discussed in Section III. The gravel A, which has a specific gravity of 3.7 and the size of 1.18-1.4 mm, are distributed around the scAUR^{TM} model as shown in Figure V.2. These tests were done under the same conditions, flume geometry, and one hour run time as the cases in Section III with a flow speed of 0.63mps at which the open bed pea gravel begins to be carried downstream.

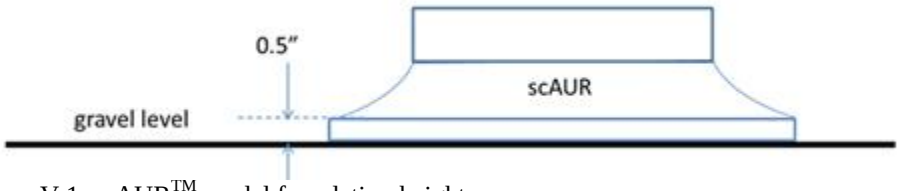

Figure V.1. scAUR^{TM} model foundation height.

For the case without a ramp, as expected, the scour occurs at the front corners of the model due to the front foundation horseshoe vortex, as shown in Figures V.3 and V.4. There is a gravel accumulation along the pier side near the location of VGs on the scAUR^{TM} model fairing on the pier, which is caused by the vortices and downstream upflow generated by these VGs. In a flood, the front of the foundation would continue to scour until some equilibrium depth would occur, such as shown for rectangular piers in (*8, 12)*. If the foundation height is too small for the rate of scour, scour under the foundation would be possible, which could weaken the structure under the foundation.

For the case for the 0.5" (12.7mm) high foundation with a curved-top ramp with a wider leading edge than its downstream edge with the foundation (trapezoidal planform), the scour occurred at the front corner of the ramp and

more gravel accumulates along the pier side around the VGs (*8*). Furthermore, there is a gravel mound at the downstream model edge. It seems that the gravel carried from the upstream are accumulated along the pier side and at the pier end. Therefore, the tested trapezoidal planform front ramp is not effective to reduce or prevent the scour when the edge of the foundation is higher than the surrounding bed.

For the 0.5" (12.7mm) high elevation with 0.75" (19mm) high curved-top straight-sided rectangular planform ramp, the front scour is negligible since the ramp is submerged 0.25" (6.35mm) and the blunt nose of the ramp is not exposed to the flow. The scour hole and mound along the side is also minimized. The scour hole along the pier side is away from the pier foundation several pier heights and the gravel accumulate on the pier side downstream of the VG. Results for a 0.75" (19mm) high foundation produced very similar results (*8*). In summary, all of these foundation tests show that a leading edge curved-top rectangular planform ramp will prevent scour around a foundation when there is open bed scour.

In order to understand how the curved-top leading edge straight-sided ramp will be effective in practice, let us consider a likely typical scenario of the scour during a flood. When installed, the curved leading-edge straight-sided ramp would be submerged beneath the surrounding bed material. The bed material would be placed around the foundation with its top surface flush with the edge of the foundation. As the flood water speed increases, open-bed scour will occur first. The bed material next to the foundation will scour at a lower rate. As the curved-top rectangular planform ramp begins to be exposed during the flood, the ramp side edges each creates a stream-wise vortex with a sense that pulls the bed material toward the foundation. This prevents the level of the bed material next to the pier side from decreasing, which prevents undermining of the material that provides structural support for the pier.

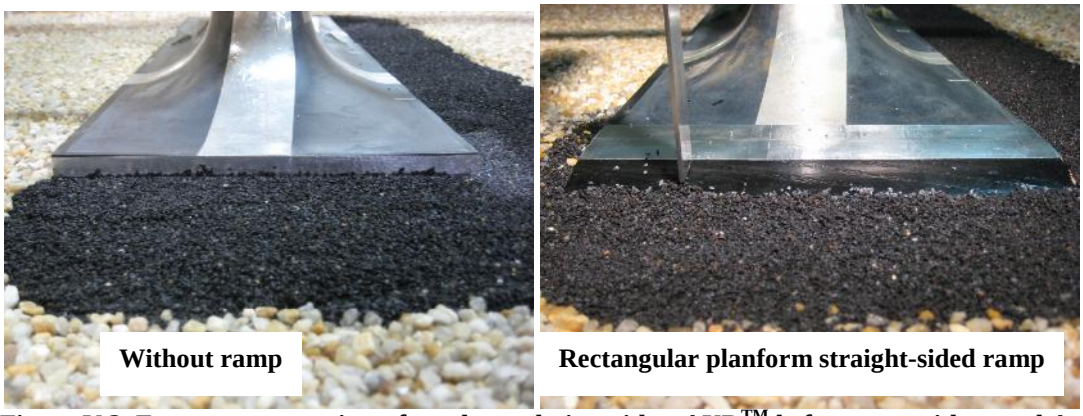

Figure V.2. Front upstream view of an elevated pier with scAUR™ before tests with gravel A of 1.18-1.4 mm in size. The foundation height is 0.5" (12.7mm). Note that the straight-sided curved top ramp is 0.75" (19mm) high and is buried 0.25"(6.35mm) under the gravel in order to make the downstream ramp edge flush with scAUR™ surface and to submerge the blunt leading edge of the curved ramp.

Figure V.3. Gravel level after flume test for 0.5" (12.7mm) high elevation <u>without a leading edge ramp</u>. Note laser sheet for gravel surface measurement. Note scour at the front corners of the foundation.

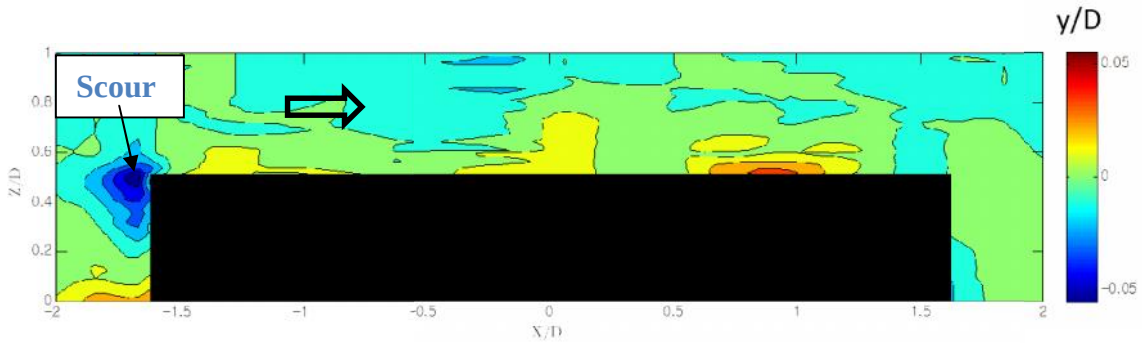

Figure V.4. Contour of gravel A bed level difference between before and after the flume test for the 0.5" (12.7mm) high elevation without a leading edge ramp. Bottom of figure is model centerline.

Figure V.5. Gravel level after flume test for 0.5" (12.7mm) high elevation with a 0.75" (19mm) high curved-top rectangular planform straight-sided leading edge ramp buried 0.25" (6.35mm) in the gravel. Note very little scour around the foundation.

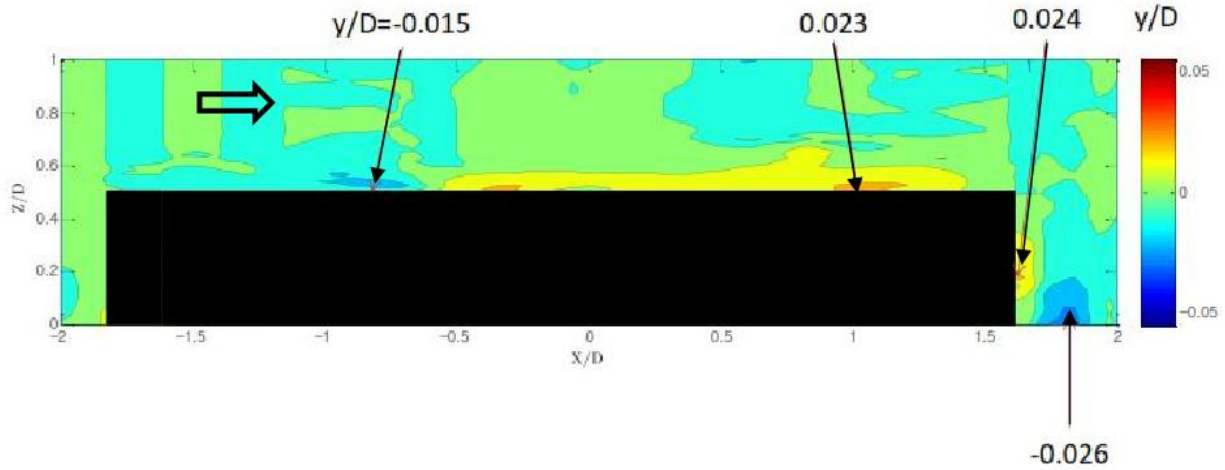

Figure V.6. Contour of gravel A bed level difference between after and before the flume test for a 0.5" (12.7mm) high elevation with a 0.75" (19.1mm) high curved-top rectangular planform leading edge ramp buried 0.25" (6.4mm) in the gravel. No scour observed within measured uncertainties of y/D = +/- 0.007. Bottom of figure is model centerline.

VI. DESIGN AND CONSTRUCTION OF A FULL-SCALE scAUR™ AND VorGAUR™ PIER MODEL

A full-scale scAUR™ and VorGAUR™ pier model was designed and constructed for testing in a large flume. Figure VI.1 shows a drawing of the wooden skeleton of the full-scale scAUR™ test model with identical nose and stern sections and 3 side sections on each side. Figure VII.1 below is a photo of the assembled test model with the sheet metal skin in a large flume. This scAUR™ full-scale model was mounted around a full-scale 1.5' (0.457m) wide and 27.5 ' (8.38m) long pier model that has a circular nose and circular stern.

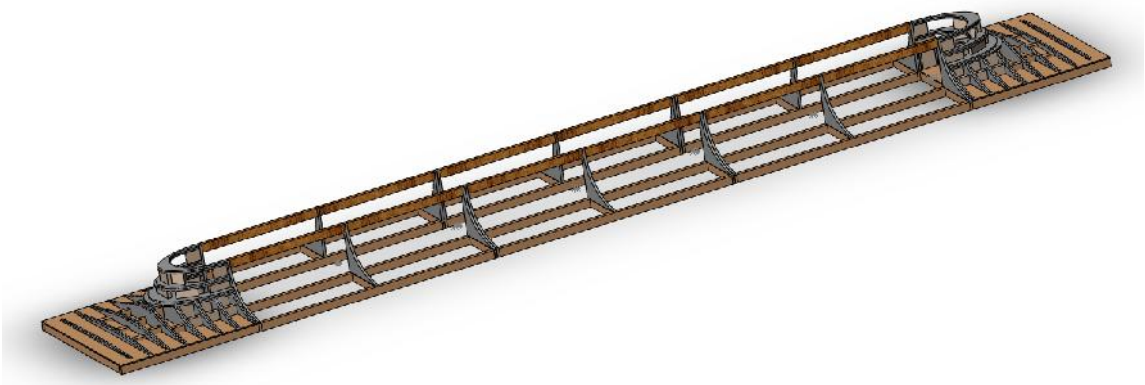

Figure VI.1. Perspective view of the full-scale scAUR™ model skeleton. The nose and stern sections are the same, while each of the 6 side sections are the same. Total model length is 400 inches. Model covered with sheet metal skin.

VII. FULL-SCALE TESTING OF SCAUR™ AND VORGAUR™ PRODUCTS IN THE UNIVERSITY OF IOWA INSTITUTE OF HYDRAULIC RESEARCH (IIHR) FLUME

Full-scale pier model scour tests were conducted during May 20-24, 2013 in the University of Iowa Institute of Hydraulic Research (IIHR) Environmental Flow Facility (EFF). Information regarding this flume and flow capabilities is at: http://www.iihr.uiowa.edu/research/instrumentation-and-technology/environmental-flow-facility/. Previously measured inflow velocity profiles validated the high quality of flow in this flume, which increased confidence that high quality and unquestionable scour data would be obtained. The full-scale model discussed in Section VI above was attached to steel channel that was screwed to the flume floor to prevent floatation.

Two test gravel sediment sizes (specific gravity = 3) that were available in Iowa City, Iowa were used during each test. With only a trace amount below 1/8" (3.2mm), by weight about 63% of the smaller sediment gravel was between 1/8" (3.2mm) and ¼" (6.4mm) and 37% was between ¼" (6.4mm) and 3/8" (9.5mm). For this smaller gravel, the weighted average size is $d50$ = 0.23" (5.94mm) and a $t/d50$ = 77. The smaller gravel was located near the front on the left side of the model facing downstream. The larger test gravel, which filled most of the flume bed, was between 3/8" and 5/8", which is $t/d50$ = 36.

Five full-scale model configurations were tested with the larger and smaller gravel on opposite sides of the model:
Configuration A: Full-scale scAUR™ with 6 VorGAUR™ vortex generators with 3 side sections on each side, as shown in Figures VI.1 and VI.2 below.
Configuration B: Full-scale scAUR™ with 8 VorGAUR™ vortex generators with 3 side sections on each side.
Configuration C: Full-scale scAUR™ with 8 VorGAUR™ vortex generators with 3 side sections on each side and the leading edge curved-top rectangular planform ramp, but with the model 3" (76.2mm) above the surrounding gravel bed.
Configuration D: Full-scale scAUR™ with 8 VorGAUR™ vortex generators with 1side section on each side.
Configuration E: Full-scale scAUR™ nose and tail sections with 4 nose section VorGAUR™ vortex generators with no side sections.

Configuration A was tested to examine the full-scale flow and scour behavior for a pier width to length ratio similar to candidate scour-critical bridges. After it was observed that some of the smaller gravel scoured downstream of the model for the Configuration A test, another vortex generator on each side of the pier was added for Configuration B to try to move more flow upward near the model end and reduce scour. Because the curved-top rectangular planform leading edge ramp was useful in preventing scour around foundations exposed by open-bed scour in the AUR small model flume studies (Section V above), Configuration C was tested. Configuration D was

selected to examine the effect of pier width to length ratio on scour for cases where multiple circular piers in a row could be surrounded by one scAUR^{TM} fairing. Configuration E examines scour for the case where a scAUR^{TM} fairing is around one nearly circular pier. The small and large gravel bed sections are flush with the edge of the model for all configurations, except Configuration C when the model is elevated 3" (76.2mm) above the bed to simulate a foundation exposed by open bed scour. The flume test section water level was 36" (0.914m) above the test bed and the near-free-surface flow speed was about 30 inches/sec (0.76m/s) for all Configurations, since "open-bed "scour of the smaller gravel was observed at this speed.

A 3.5" (88.9mm) outside diameter vertical circular cylinder model was located downstream of the scAUR^{TM} model about 18" (457mm) from a flume side wall and 18" (457mm) from the end of the gravel bed and tested with the larger gravel at the same time as each of the several configurations of the scAUR^{TM} full-scale model to show that the flow conditions cause scour with the cylinder. Test runs continued until after the cylinder scour reached equilibrium conditions with no further observed scour; longer runs are noted when they are discussed below. With the larger gravel, the equilibrium scour hole was 3" (76mm) deep in front of the cylinder and extended 3.5" (89mm) upstream with a span-wise width of 11" (0.28m).

Measurements that were obtained included the scour depth around the base of the model after the flume was drained using photos of laser sheet surface locations (*12),* surface oilflows over the model to determine the local surface flow direction, and some pitot tube flow velocity data in front of and around the model. Unfortunately, the water was too muddy to obtain underwater photos and videos, although open bed scour could be observed through the glass flume side wall using an intense light.

For Configuration A, no scour was observed around the model except downstream of the scAUR^{TM} fairing in the smaller gravel (Figure VII.3). The downstream scour hole shown in the right photo of Figure VII.4 is about 1" (25.4mm) deep and 4' (1.22m) long. Surface oilflows show that the near surface flow moves up the scAUR^{TM} fairing just downstream of the VGs, as desired, but further downstream after separation, the flow moves down *(8)*. Large-scaled vortices are shed from the rear of the model and cause the scour of the smaller gravel. Scour of the larger gravel was observed around the 3.5" (89mm) diameter circular cylinder (Figure VII.5) for all the configurations, taking about 20 minutes to reach equilibrium.

In order to try to reduce the size of the separation region and intensity of the large-scaled separated flow, a fourth VG on each side was added for the Configuration B test. The upstream end of the added fourth VG on each side of the model for Configuration B is located at 30 inches (0.762m) above the bottom of the scAUR^{TM} model while the downstream end is 33 ¼" (0.845m) from bottom at the same stream-wise location as the other 3 VGs on each side. Again, the test showed no scour around the upstream and sides of the scAUR^{TM} model or anywhere with the larger gravel, but again scour of smaller gravel occurs downstream of model. Figure VII.6 shows the contours. This scour hole is about 2" (50.8mm) deep, 18" (0.457m) wide and 2' (0.610m) long from a test time of 30 minutes, long after the scour hole around the circular cylinder ceased to scour more and reached equilibrium at 20 minutes.

The rectangular planform leading edge ramp for Configuration C is shown in the left photo of Figure VII.7. Like the earlier AUR flume tests (Section V) with an exposed foundation due to open-bed scour, this straight-sided curved ramp prevented scour around the upstream and sides of this exposed foundation *(8)*. Like Configurations A and B, there was scour of the smaller gravel downstream of the scAUR^{TM} model, as shown in Figure VII.8. This scour hole was about 1" (25.4mm) deep from 3' (76.2mm) to 8' (2.44m) from the downstream edge of the model after a 58 minutes run. The deposition mound was about 1.5" (38.1mm) high, stretching from 8' (2.44m) to 13' (3.96m) from the model.

For Configuration D, there is no scour around the front or side of the model. The downstream scour hole for a 35 minutes run at a slightly higher speed of 33inches/sec (0.84 m/sec) is deeper than Configurations A, B, and C. The apparent scour of the larger gravel near the centerline is due to larger gravel rolling into the hole created by scour of the smaller gravel.

For Configuration E, there is no scour around the front or side of the model or where there is the larger gravel downstream. For a 32 minutes run at a slightly higher speed of 32 inches/sec (0.813m/s), the downstream smaller gravel scour hole is about 3" (76.2mm) deep, 28" (0.711m) wide, and 36" (0.915m) long. The gravel are deposited about 36" (0.915m) to 60" (1.52m) downstream from the end of model. The downstream smaller gravel scour hole is similar to that for Configuration D. The apparent scour of the larger gravel near the centerline is due to larger gravel rolling into the smaller gravel hole. **IIHR staff members witnessed each test and signed statements that they observed the results that are reported here.**

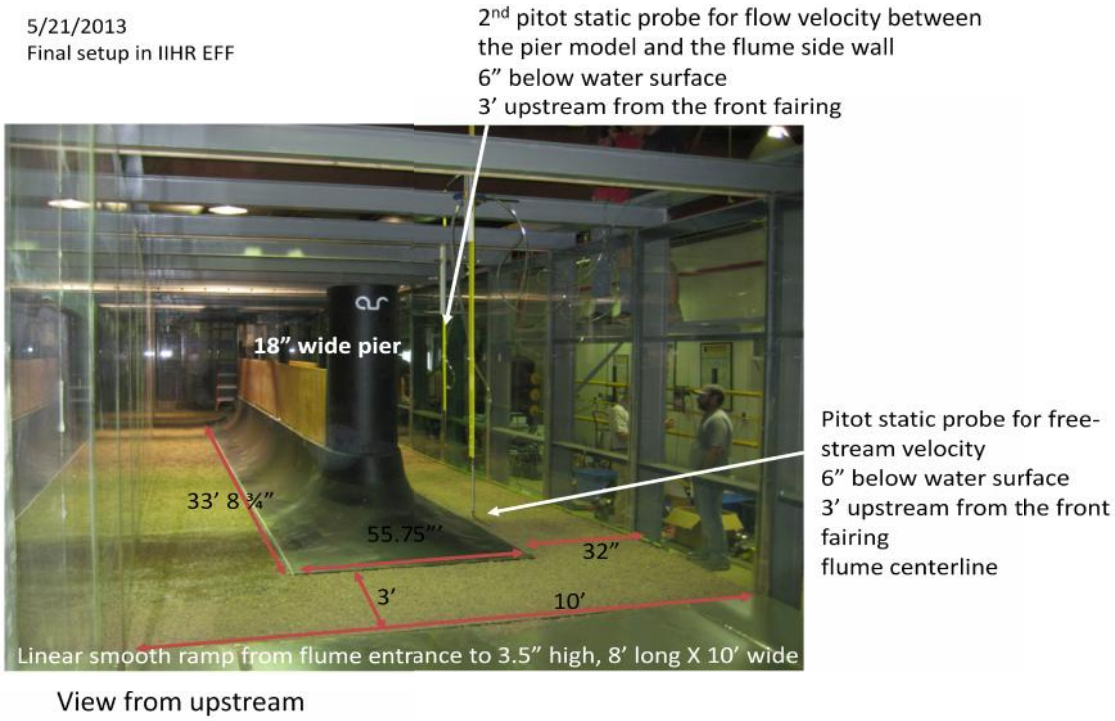

Figure VII.1. Photo from upstream of the AUR full-scale scAUR™ with VorGAUR™ vortex generators model in the IIHR Environmental Flume Facility with 3 side sections on each side for Configurations A and B. Small and large gravel are flush with the edge of the model. An 8' (2.44m) long upstream approach ramp from the flume entrance floor to the sediment bed and a downstream sediment collection basin were used.

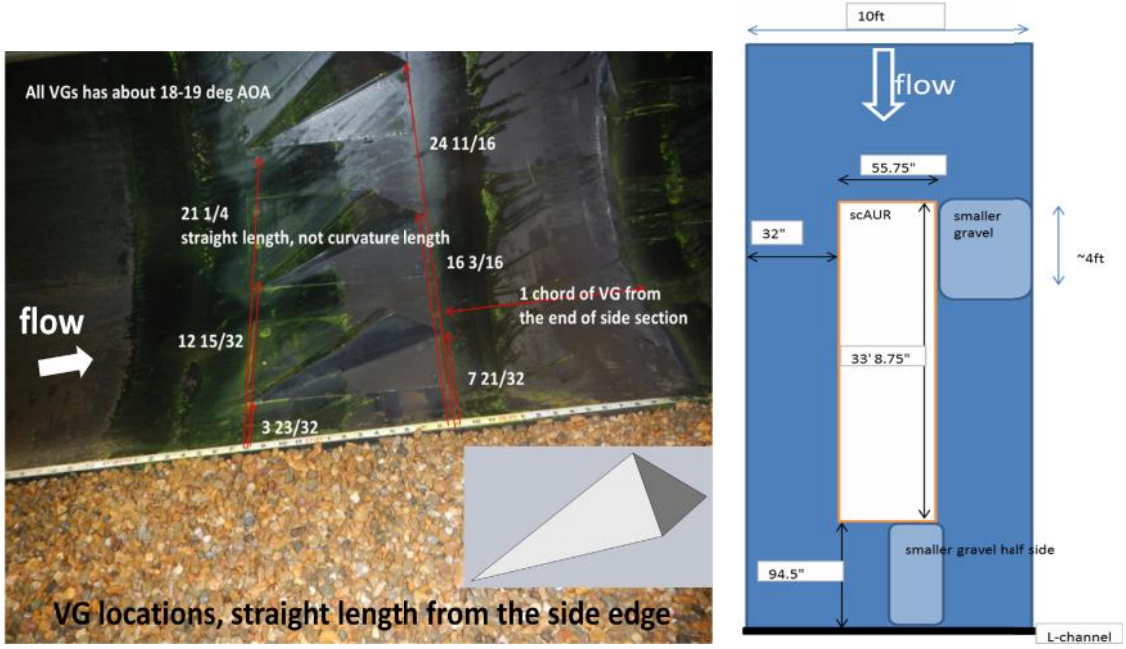

Figure VII.2. (left) Photo of the locations (in inches) of the bottom 3 VorGAUR™ vortex generators near the end of each downstream side section for Configurations A, B, C, and D. Inset drawing of the VorGAUR™ vortex generators that are 3.5" (88.9mm) high by 14" (356mm) long. (right) Plan view of locations of the AUR full-scale scAUR™ with VorGAUR™ vortex generators model and small and large gravel beds for Configurations A, B, and C.

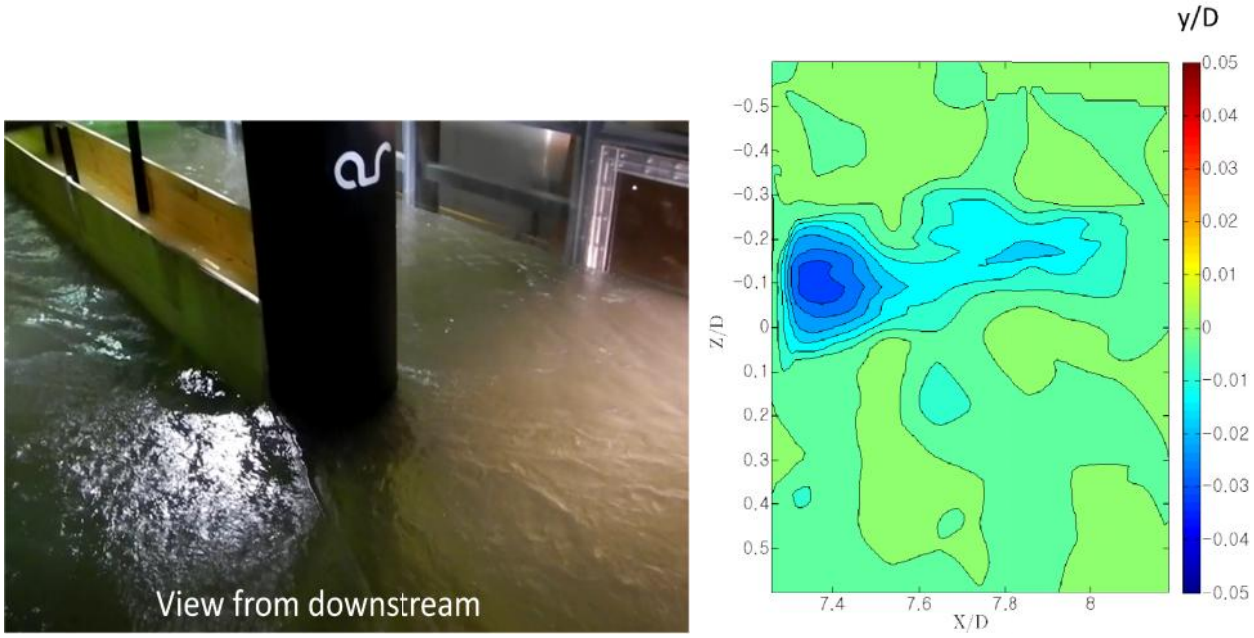

Figure VII.3. (left) Photo of flume surface flow for Configuration A showing separation at the downstream end of the pier. (right) Contours of scour downstream of model for Configuration A; left edge of contour is at model downstream edge. No scour of larger gravel. X (streamwise), Y (scour depth), and Z (spanwise) co-ordinates are normalized on D, the scAUR™ model width at the bottom, 55.75" (1.416m).

Figure VII.4. Configuration A: no scour of small or large gravel around front and sides of full-scale scAUR™ model with 6 VorGAUR™ (left); scour of smaller gravel downstream of model (right). Flow from right to left.

Figure VII.5. Surface bow wave around the 3.5" (88.9mm) diameter comparison circular cylinder during a test (left). Equilibrium large-sized gravel scour hole in front of 3.5" (88.9mm) diameter circular cylinder and laser sheet (right); typical for tests for all Configurations.

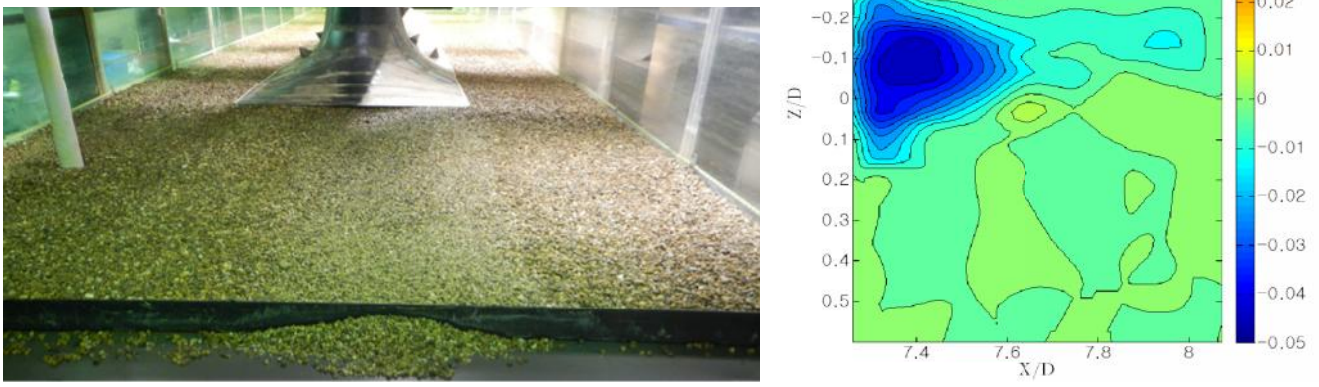

Figure VII.6. Configuration B: no scour of small or large gravel around front or sides of full-scale scAUR™ with 8 VorGAUR™ VGs; scour of smaller gravel occurs downstream of model (a, left). (b, right) Contours of scour downstream of model for Configuration B; left edge of contour is at model downstream edge. No scour of larger gravel.

Figure VII.7 Configuration C: scAUR™ full-scale model with 8 VorGAUR™ VGs raised 3" above gravel bed with leading edge ramp (left). Looking downstream (middle photo) and looking upstream (right photo).

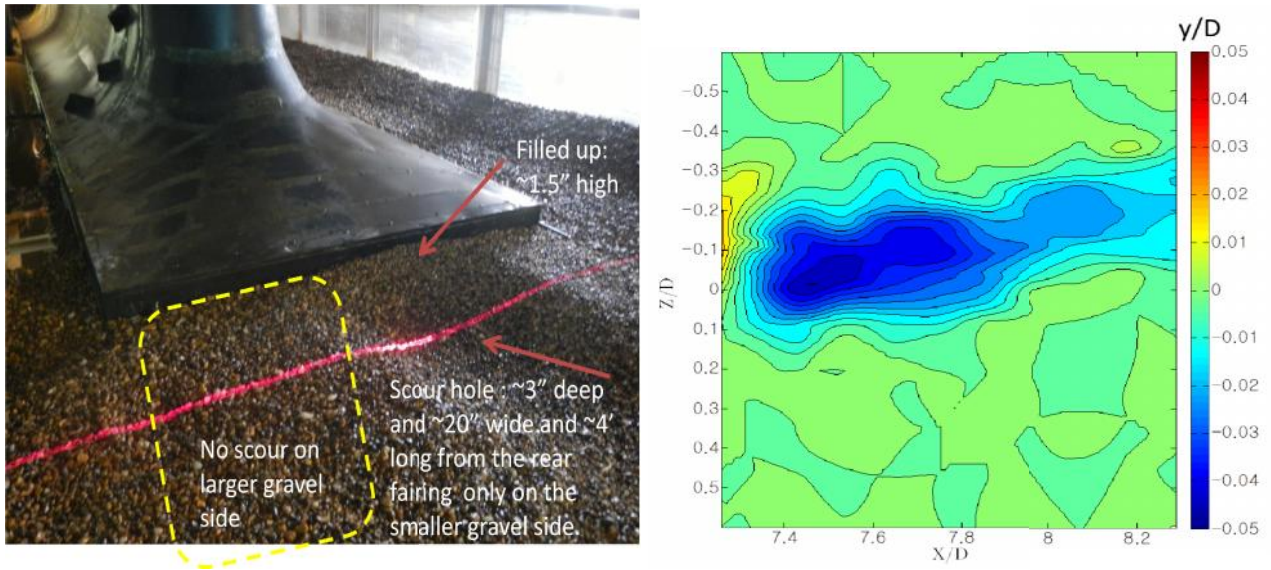

Figure VII.8 Photo of scour of smaller gravel downstream of model for Configuration C (left). Scour depth contours (right).

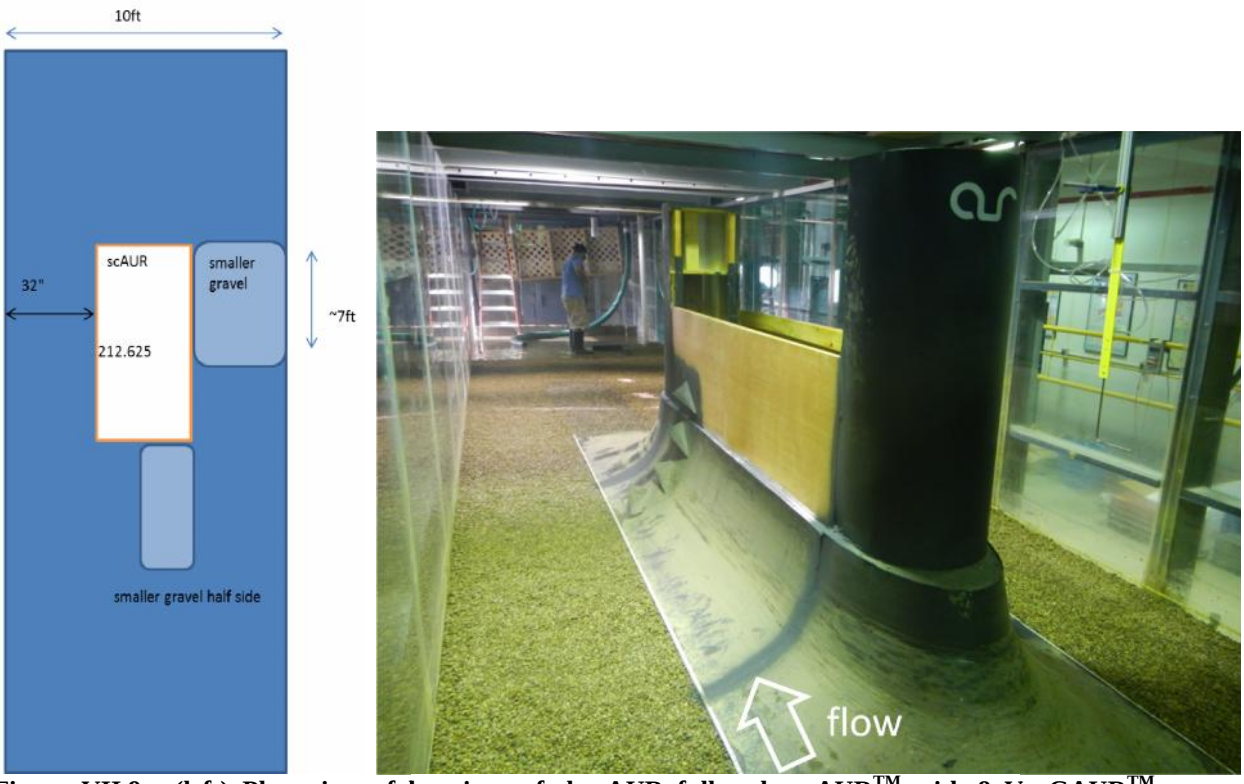

Figure VII.9. (left) Plan view of locations of the AUR full-scale scAUR™ with 8 VorGAUR™ vortex generators model and gravel beds for Configuration D with one side section on each side. (right) Photo of full-scale model and 4 VGs on one side. Note that the gravel bed is level with the model edge.

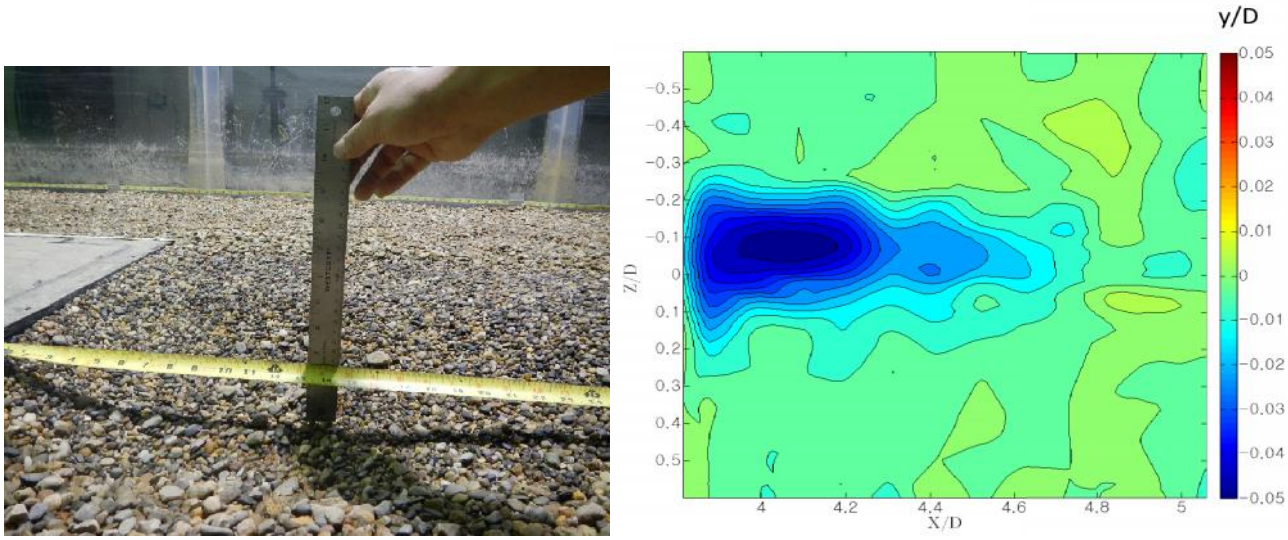

Figure VII.10. Photo of scour of smaller gravel downstream of model for Configuration D (left). Scour hole is up to 2.5" (62.5mm) deep, 2' (0.610m) wide and 45"(1.14m) long. Scour depth contours (right).

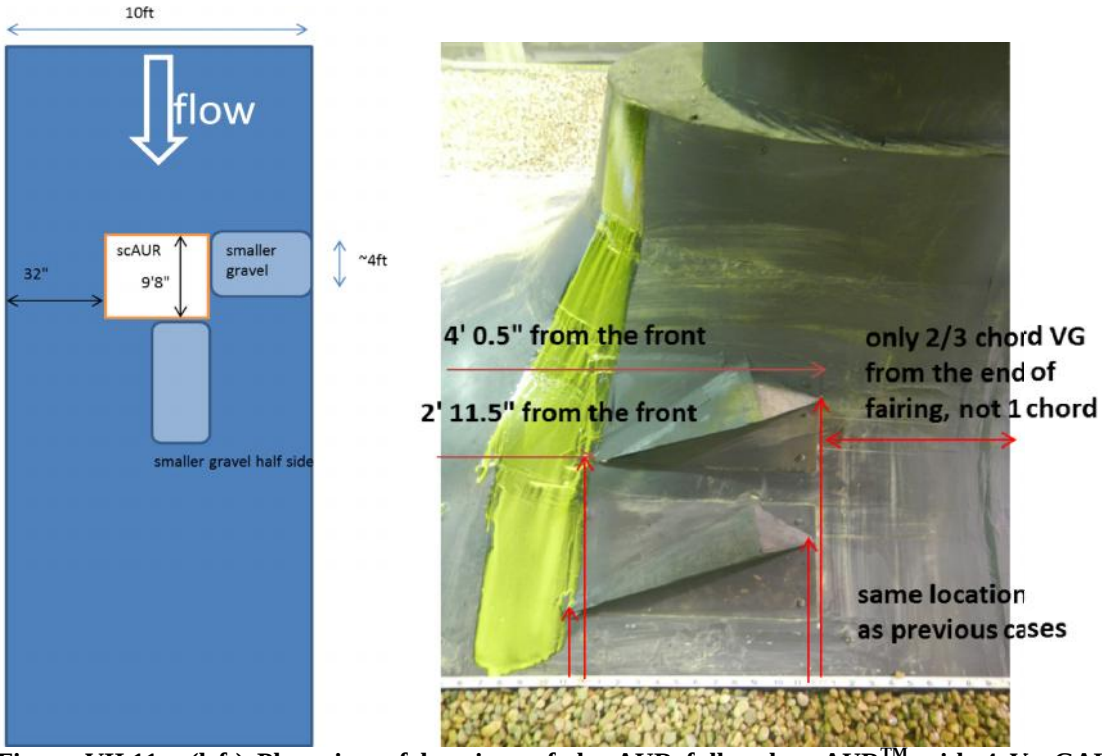

Figure VII.11. (left) Plan view of locations of the AUR full-scale scAUR™ with 4 VorGAUR™ vortex generators model and gravel beds for Configuration E with no side section on each side. (right) Photo of full-scale model and 2 VGs on one side. Note that the gravel bed is level with the model edge.

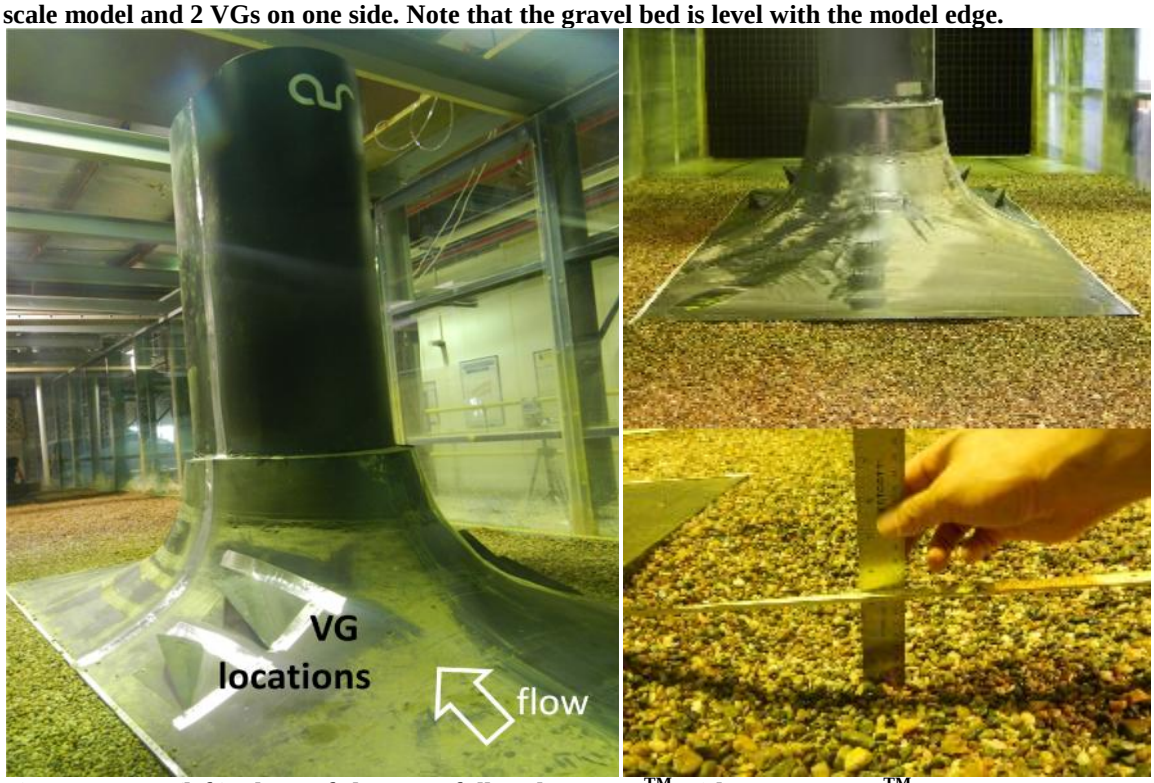

Figure VII.12. (left) Photo of the AUR full-scale scAUR™ with 4 VorGAUR™ vortex generators model and gravel beds for Configurations E with no side section on each side. (right) Photos of downstream small gravel scour.

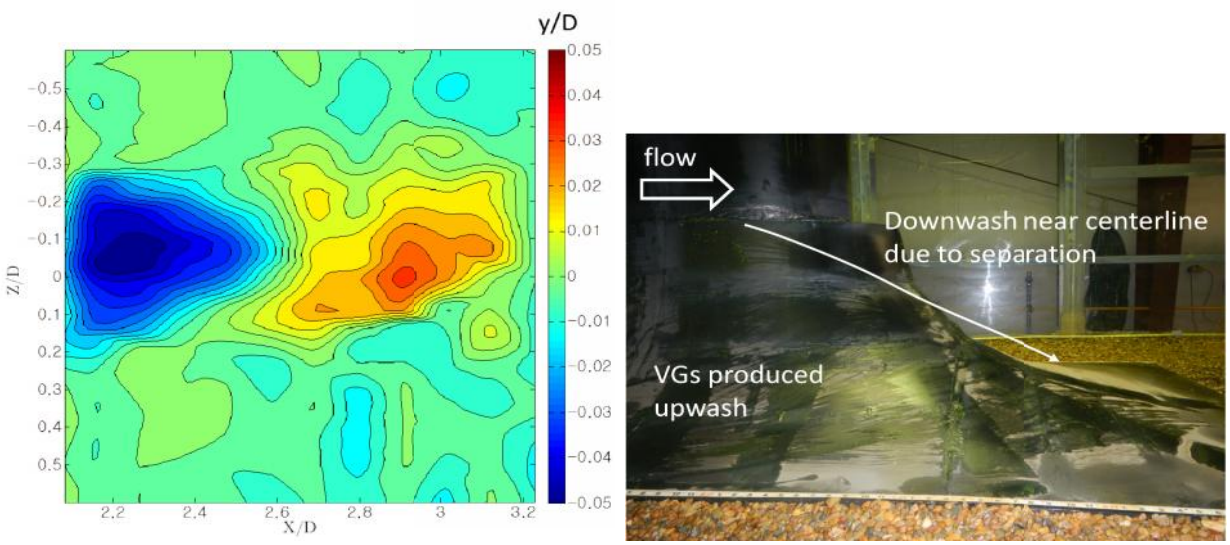

Figure VII.13. (left) Contour plot of scour depth downstream of model for Configuration E. (right) Oilflow showing upwash due to the VGs and a near centerline downwash due to separation.

In summary of these tests, the full-scale model tests confirmed that there was no scour around the front and sides of each of the Configurations with either the smaller or larger gravel, as was also observed at model scale. However, all 5 of the Configurations showed scour of the smaller gravel downstream of the model in similar patterns with depths about proportional to the run time. Scour at this location was not observed in the model-scale flume runs where the model width to flume width is 1/16. All of this downstream scour for all of the full-scale test Configurations can be explained by the fact that stronger adverse or positive pressure gradients that induce premature separation of the boundary layer and large-scaled flow recirculation are present at the downstream end of the model due to flow blockage effects in the IIHR EFF flume than were present in AUR model scale tests.

Because the full-scale model pier width (1.5' or 0.457m) to IIHR EFF flume width (10' or 3.05m) was 0.15 and the bottom of the model width to flume width was 0.46, there are significant flow blockage effects *(13)*. Calculations and AUR model flume experiments were performed by AUR Staff to assess the effect of model blockage on the flow *(8)*. The AUR small flume model (3" or 76.2mm wide pier) was located in the center of a 20" (0.508m) wide AUR flume as shown in Figure VII.14 to produce the same model flow blockage as in the IIHR full-scale tests *(8)*. The smallest black sediment gravel A used in Section III, 1.08-1.14mm diameter, was distributed around the model because the previous 48" (1.22m) wide AUR flume test with the sediment A did not show any scour around the model.

The upstream flow speed was set to 22.8 in/sec (0.58m/s) and the corresponding flow speed on the side increased about 9-10%. Note that there was about 40% increase of speed on the side of the model at IIHR. After a 50 minutes run of the small flume, scour holes on opposite sides of the model centerline were generated downstream of the small flume model like the IIHR full-scale test with the smaller gravel, as shown in the photo and contour plot in Figure VII.14 Another test with the same flow geometry and situation, but with a NACA 0024 airfoil tail mounted on the model stern to produce weaker adverse pressure gradients around the stern, **generated no scour downstream**, supporting the idea that blockage effects produce stronger adverse pressure gradients, stronger separation regions and thus scour *(8)*. **It is clear from all of these tests that the downstream scour of the smaller gravel that was observed in the IIHR full-scale model test was due to the flow blockage effect of the AUR full-scale model in the IIHR flume.**

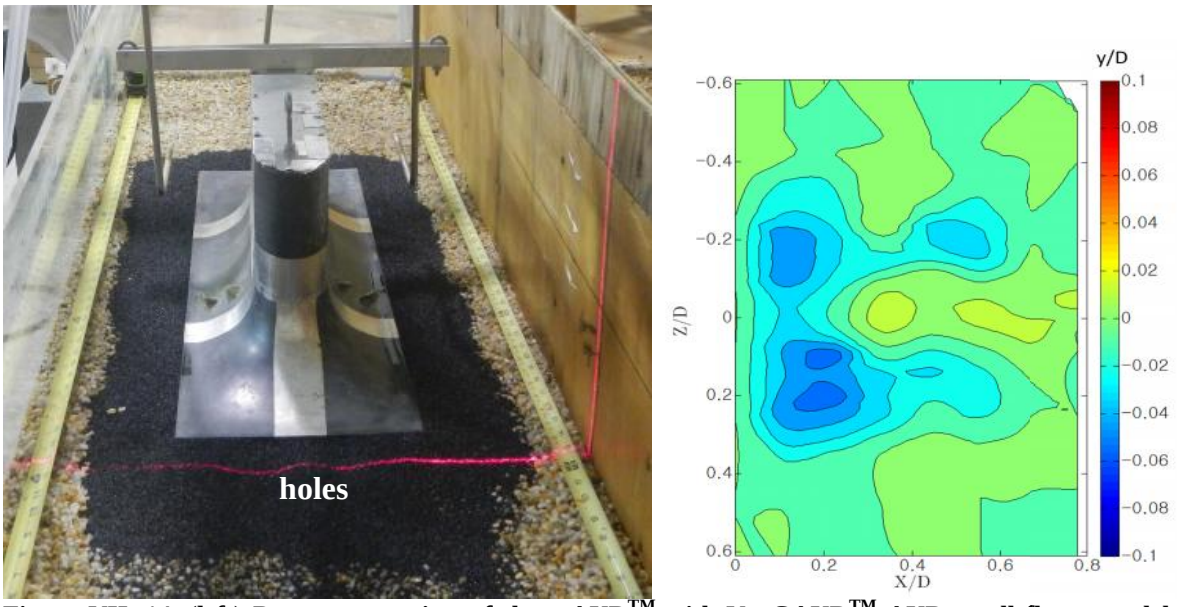

Figure VII. 14. (left) Downstream view of the scAUR™ with VorGAUR™ AUR small flume model (3" or 76.2mm wide pier) located in the center of a 20" (0.508m) wide AUR flume to produce the same model flow blockage as for the full-scale IIHR tests *(1)* with the smallest black sediment A, 1.08-1.14mm diameter, distributed around the model. Note the laser sheet on downstream scoured sediment and holes. (right) Contour of scour depth. Left edge of contour is at model downstream edge. Note x/D=0 at the end of the model, Max y/D=0.02 and Min y/D=-0.05

VIII. REFINED MANUFACTURING PROCESSES AND COSTS FOR SCAUR™ AND VORGAUR™ PRODUCTS

The next phase of developing the practical use of these innovations is to develop specific plans for the prototype manufacture and installation of full-scale scAUR™ and VorGAUR™ products on at least one pier and one abutment for a selected scour-critical bridge in Virginia that has a record of flooding and is representative of scour-critical bridges across America. The selection of a scour-critical bridge in Virginia is discussed in Section I, while the manufacturing and installation processes are discussed here and in Section IX below. In order to further reduce costs and increase the versatility of the scAUR™ and VorGAUR™ products, multiple manufacturing alternatives were considered. The required labor, materials, time, logistics, and practical issues were examined and used to evaluate the possibility of adjusting manufacturing plans from the earlier AUR manufacturing and cost study. AUR considered many details for the various manufacturing alternatives (*8*), but only the key ideas on which decisions are made are discussed and summarized here.

Retrofit to an Existing Bridge

One approach is to use pre-cast or cast-in-place concrete scAUR™ components. A foam master male mold for creating a master fiberglass female mold shaped for pre-cast and cast-in-place concrete scAUR™ components was used earlier *(8).* AUR has built prototype scAUR™ pre-cast components, so the process and costs are known. "Shotcrete" also was examined as an approach to constructing a concrete scAUR™ fairing as a retrofit to a bridge. However, there are many sources of failure and the shotcrete process is not a cheaper alternative to pre-cast concrete when the uncertain product shape quality and the likelihood of correcting mistakes are considered. It would require the design and development of an accurate laser sheet measurement system to ensure sufficient scAUR™ shape fidelity, development of training methods for skilled and expensive technicians for field installation, development of methods for various field environmental conditions, continual quality control oversight, and anticipation of many uncertainties that would require reserve approaches as well as methods to correct errors *(8).*

An attractive manufacturing alternative for a scAUR™ retrofit bridge fairing is to use stainless steel (SS) or even weathering steel. Stainless steel was considered for both the double curvature end sections and the cylindrical sides of the scAUR™. Its corrosion resistance gives it a lifetime of 100 years even in seawater environments, using a proper thickness, construction methods, and type of SS. It is an effective way to reduce weight and the cost associated with casting custom reinforced concrete structures. Another benefit is that the SS VorGAUR™ vortex

generators could be welded directly onto the side sections instead of having to be integrated into the rebar cage of the reinforced concrete structure.

Typical example costs for each of these manufacturing approaches were developed from current cost information and quotations from concrete and steel fabricators *(8)*. Table VIII.1 is a cost comparison for example piers of various widths and 32 feet (9.76m) long. For larger piers, the costs for stainless steel and shotcrete vary about with the square of the pier width times the pier length. Precast concrete costs for larger piers vary with the pier width to the exponential power of 2.3 times the pier length. A similar cost study for abutments, like the one shown in Figure VIII.1, also shows similar relative costs for the 3 approaches. The total cost for a SS retrofit for a 32' (9.76m) long spill-through or wing-wall abutment is $25K. These estimates include all costs of fabrication of components and molds, materials, labor, transportation, installation, and finish work, such as painting the stainless steel with an approved concrete colored paint. Costs for overhead, G&A, and profit are not included. **It is clear that stainless steel is the best choice for bridge retrofits.**

	Pier Width (ft)					
	1.5	2	3	4	5	6
Stainless Steel (304L)	$ 22,000	$ 32,000	$ 62,000	$ 100,000	$ 160,000	$ 220,000
Precast	$ 33,000	$ 56,000	$130,000	$230,000	$380,000	$580,000
Shotcrete	$ 30,000	$47,000	$ 96,000	$160,000	$ 250,000	$350,000

Table VIII.1. Comparison of estimated TOTAL retrofit costs for one pier of various width 32' long piers for several approaches.

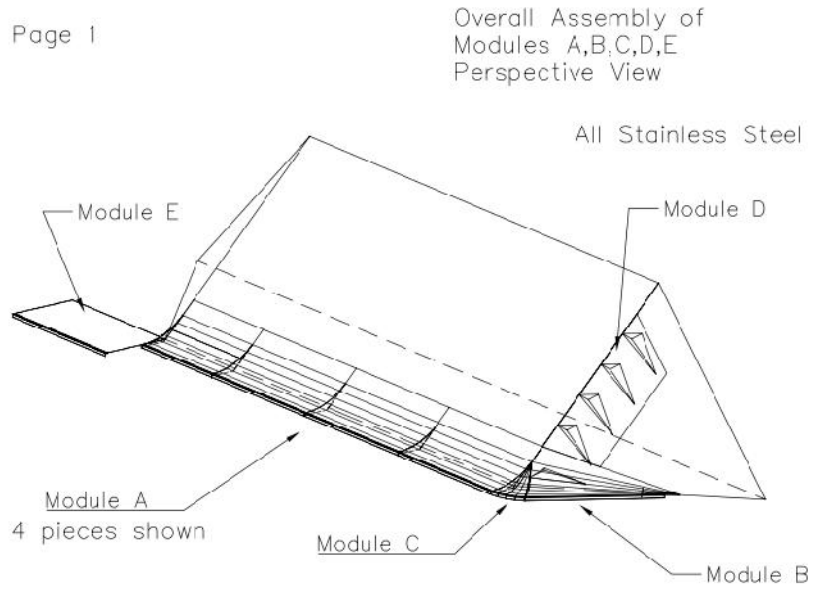

Figure VIII.1. Example stainless steel scAUR^{TM} retrofit for a spill-through abutment.

New construction

In the case with new construction, essentially the difference between the way cast-in-place bridge piers and abutments are constructed currently without the scAUR^{TM} products and in the future with the scAUR^{TM} products is that scAUR^{TM} steel forms for the concrete are used *(8)*. All standard currently used concrete construction methods and tools can be used. During the bridge design phases, the bridge pier or abutment foundation or footer top surface width and length would need to be large enough to accommodate the location of the scAUR^{TM} concrete fairing on top. Rebar needed for the scAUR^{TM} would be included in the foundation during its construction. Stainless steel rebar for welding to the stainless steel vortex generators mounting plates on the surface need to be used for specific locations.

Standard methods for assemblying forms and pouring the concrete will be used, as discussed in (*8)* and ACI 318-11. The contractor simply needs to replace the currently used forms for the lowest level of the pier above the foundation with the scAUR^{TM} forms. The scAUR^{TM} steel forms can be mounted and attached to the foundation forms *(8)*. The tops of the steel scAUR^{TM} forms on opposite sides of the pier can be attached together with steel angle to completely contain the concrete for the foundation and the scAUR^{TM} fairing. Figure VIII.2 shows an example scAUR^{TM} steel formwork. Like current methods, after the scAUR^{TM} and foundation concrete has cured sufficiently, the scAUR^{TM} and foundation forms would be removed. Currently used forms for the next higher portions of the pier or abutment can then be mounted in place for further cast-in-place concrete. Table VIII.2 shows estimated incremental costs of adding the scAUR^{TM} fairing to new construction for additional rebar, concrete, labor, scAUR^{TM} forms, and transportation of forms for various width pier construction *(8)*. Overhead, G&A, and profit is not included in these estimates. **Clearly, since the new construction cost is about 1/3 of retrofit costs, the best time to include the scAUR^{TM} fairing on piers is during new construction.**

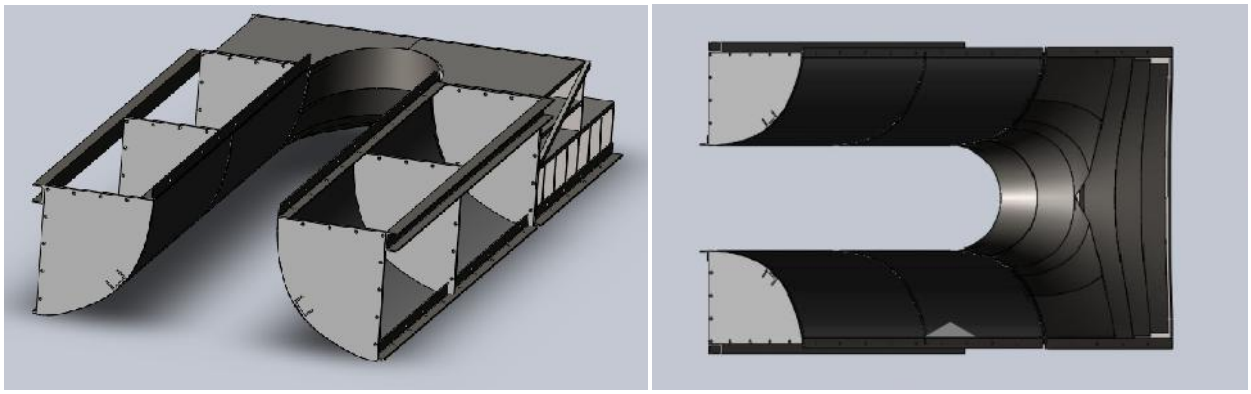

Figure VIII.2. Left, top perspective view of partial assembly (nose, 2 side sections) of steel forms for scAUR^{TM} for new concrete pier construction. Right, bottom perspective view of same partial assembly of steel forms.

	Pier Width (ft)					
	1.5	2	3	4	5	6
Cost of added materials & labor	$3,340	$ 5,690	$13,200	$25,100	$41,800	$64,100
Cost of steel scAUR form fabrication	$1,400	$2,490	$ 5,600	$ 9,960	$15,600	$22,400
Cost of form transportation (in VA)	$2,000	$2,000	$ 4,000	$ 4,000	$ 6,000	$ 6,000
Total cost for new construction	$6,740	$10,200	$22,800	$39,100	$63,300	$92,500

Table VIII.2. Estimated **incremental** total cost per pier of adding the scAUR^{TM} fairing to new 32' long concrete pier construction using scAUR^{TM} formwork. These estimates do not include overhead, G&A, and profit.

TASK IX. COMPLETE PLANS AND COST ESTIMATES FOR MANUFACTURING AND INSTALLATION OF FULL-SCALE SCAUR^{TM} AND VORGAUR^{TM} PRODUCTS FOR AT LEAST ONE PIER AND ONE ABUTMENT OF THE SELECTED REPRESENTATIVE SCOUR-CRITICAL VIRGINIA BRIDGE.

In parallel with manufacturing and installation plans discussed in Section VIII above, AUR planned for the installation of scAUR^{TM} on the scour-critical westbound Route 360 bridge over the Appomattox River and the Route 613 bridge over the Dry River, which are discussed in Section I. However, with the reasonable cost estimates for stainless steel retrofits above, any bridge anywhere can be retrofitted at a cost much less than the present value of all of the future scour monitoring, evaluation, and temporary anti-scour mitigation design and construction, usually with rip-rap (*8*).

Route 360 Westbound Bridge over the Appomattox River

Some features of this bridge were discussed in Section I. From available documents and measurements during an AUR staff visit, the width of the two 36' (10.98m) long semi-circular nose and stern piers on the westbound bridge

is about 2’ (0.61m) with a concrete footer or foundation of each pier of about 6 feet (1.83m) wide with a flat top. Although currently covered with 1’ to 2’ (0.31m to 0.61m) diameter rip-rap rocks, the east abutment of the westbound lanes appears to be a spill-though type. Figure IX.1 are a photo of the east pier on the upstream side and a photo of the east abutment covered with 1’ to 2’ (0.31m to 0.61m) rip-rap.

Figure IX.1 (left) Photo of the east pier on the upstream side of the Route 360 bridge over the Appomattox River. (right) Photo of the east abutment covered with 1’ to 2’ (0.31m to 0.61m) rip-rap. (AUR photos, April 24, 2013)

For this pier retrofit, there are a stainless steel 6 foot (1.83m) wide and 6 foot (1.83m) long nose section and an identical tail section, each weighing less than 500 pounds. Each of the identical 3 stainless steel side sections (11 feet (3.35m) in length) for each side weighs less than 300 pounds. When assembled, the inside feet of each section rest on the existing foundation of the pier next to the pier with a vertical pin in the concrete through a hole on each foot, the angle stainless steel top of each of these prefabricated SS pieces is bolted to the concrete pier using wedge anchors in the concrete pier, and all of the sections are bolted and welded together (*8).*

The side sections would be sequentially lowered by a crane from the highway above, since the surrounding river bank terrain is swampy and highly sloping. Some times of the year the river is not deep, so a cofferdam may not be needed. A cable crane or small barge under the bridge may be useful in moving the sections into position. Post welding cleaning and painting of the SS scAUR structure with an approved corrosion-resistant concrete-colored paint is recommended. This complete pier cost of all components and installation would cost about $32K. A similar installation for an abutment would cost $25K. Overhead, G&A, and profit are not included in these estimates.

Route 613 Bridge over the Dry River

The Dry River approaches the Route 613 bridge piers at about 45 degrees to the pier lengthwise centerline with massive separation around the nose during high water, as shown by earlier AUR flume experiments *(8).* Even so, AUR is able to propose a configuration of scAUR^{TM} and VorGAUR^{TM} products that prevent scouring vortices from forming around a pier on this bridge. To prevent separation around the pier nose and tail during a flood, stainless steel nose and tail extensions to the pier are proposed, as shown in Figure IX.2 below on the AUR flume model, forming a “dogleg” shape. The centerline of the pier nose and tail extensions and the nose and tail of the scAUR^{TM} are aligned with the on-coming flow direction. VorGAUR^{TM} vortex generators are used to energize the near-wall flow upstream of the adverse pressure gradient regions around the pier and prevent separation and scour.

Model scale experiments in the AUR flume were performed that confirm that this design prevents scour. The VGs are attached on both front and rear fairings as shown in Figure IX.2 below. The VGs are 3” (76.2mm) long and ¾” (19.1mm) high. The free-stream velocity is 0.58m/s and the flow speed near the VGs on the fairings is about 0.61m/s, which caused scour when the VGs were not used. As shown in the photos below, there is no scour around the model.

Manufacturing and installation processes and methods would be the same as for the Route 360 bridge described above. However the total cost of $39K for one pier is higher due to the addition of the additional components required for the SS dogleg on a pier *(8).* An abutment total cost would be about $32K, also reflecting additional costs. Overhead, G&A, and profit are not included in these estimates.

Figure IX.2. Photos of pier nose and stern additions to the AUR model used in AUR flume tests. (left) Upstream view showing location of VGs on model front right and rear left sides. (right) Laser sheet showing no scour downstream of the model.

Plans for Implementation:

Prior to this project initiation, Virginia DOT endorsed this NCHRP project and made a commitment to provide assistance for plans and to seek funds for a full-scale prototype installation after completion of this project. AUR will also contact and interact with other state DOTs.

AUR will continue to refine methodology, products, and costs to further make the acceptance, availability, and use of scAUR^{TM} and VorGAUR^{TM} products more widespread, thus making the products financially viable. AUR has the financial resources to manufacture and provide these products in the future.

CONCLUSIONS

Local scour of bridge piers and abutments is one of the most common causes of highway bridge failures *(1)*. All currently used countermeasures are temporary and do not prevent the cause of scour – discrete large-scaled vortices formed by flow separations and recirculations from the underwater structures. These large-scaled vortices bring higher velocity water down to the river bed and cause scour. Using the knowledge of how to prevent the formation of discrete vortices, prior to this IDEA project, AUR developed, proved using model-scale tests, and patented new local-scouring-vortex-prevention products (scAUR^{TM} as US Patent No. 8,348,553 and VorGAUR^{TM} as US Patent No. 8,434,723). These products prevent the near-free-surface higher velocity water from going down to the river bottom and cause scour. These products keep the lower velocity water near the river bed. These are practical long-term cost-effective permanent solutions to the bridge pier and abutment local scour problem, no matter what types and sizes of soil and rocks surround the pier or abutment.

In this current NCHRP Project, further computational work on the effect of pier size or scale and model flume tests for other sediments, for other abutment designs, and for a curved-top rectangular planform leading edge foundation ramp under open bed scour conditions showed that the products prevent scouring vortices and scour. Full-scale prototypes of these proven products were successfully tested and very cost-effective manufacturing and installation plans were developed for a representative scour-critical bridge Virginia.

These results strengthened the payoffs for practice that were identified in the earlier AUR work. In addition to permanently preventing the formation of local scouring vortical flows due to flow separation around bridge piers and abutments of any width to length ratio that cause local scour for any size or scale bridge pier or abutment, the scAUR^{TM} with VorGAUR^{TM} designs are effective for swirling and large angle-of-attack approach flows. There are lower drag forces on the bridge because no high speed water is drawn down to the pier or abutment surface, much lower flow blockage since the water is accelerated around the pier or abutment, much lower water level since the flow is more accelerated around the pier or abutment, and much lower over-topping frequencies on bridges during flood conditions because the water moves faster around the bridge, for any water level or turbulence level.

In the earlier AUR work, the scAUR^{TM} with VorGAUR^{TM} designs were shown to prevent debris accumulation and provide protection from impact loads because of the streamlined flow around the pier without a horseshoe vortex, which deflects objects and debris away from the underwater structure. For a piece of debris to remain lodged in front of a pier would require perfect balance of the debris weight on both sides of the pier. The scAUR^{TM} shape with VorGAUR^{TM} prevents the formation of the pier nose horseshoe vortex, so there is no downflow at the pier that

would submerge the floating debris. In reality, the bow wave in front of a pier is unsteady, meaning that the position of an arbitrary piece of debris is unstable to asymmetries of the flow. Thus, the debris would move to one side of the pier or the other and float downstream. The vortex generators are designed so no debris can get caught. The downstream sloping surfaces of the VGs have no place to catch the debris. Vortex generators around the nose of the pier or the upstream edge of an abutment create counter-rotating vortices that diffuse the free-surface pier bow or abutment separation vortex, greatly reduce the downwash from these vortices, and prevent scour on the river bed.

There will be more stability for the soil and rocks surrounding the piers and abutments when the scAUR^{TM} shape with VorGAUR^{TM} and leading edge ramp are used. Scour generated around a scAUR^{TM} with VorGAUR^{TM} protected foundation always occurs at a significantly higher approach flow speed than a speed that will cause open-bed scour. Huge flow speeds will cause open-bed scour but the curved-top rectangular planform leading edge ramp creates counter-rotating vortices on each side that bring open-bed materials toward the foundation for protection from further scour.

Such piers and abutment protected with scAUR^{TM} with VorGAUR^{TM} and a curved-top rectangular leading edge foundation ramp can have 100 year or more lifetimes and longer bridge life. Since loose open-bed scoured material will be brought toward the sides of the pier or abutment, the bottom of the foundation will always have material around it, even if an upper portion of the foundation is exposed because of high speed flood waters. The lifetimes of the scAUR^{TM} with VorGAUR^{TM} products are dictated by their construction materials, such as the thickness of the stainless steel for retrofits and the quality of the concrete for new construction. High quality proven-technology prefabricated stainless steel or cast concrete components are used for quality control, rapid installation, and lowest cost. The present value cost of these products over the life of a bridge are an order of magnitude cheaper than current scour countermeasures.

Virginia DOT has committed to seek funds to install prototype products on a bridge. AUR will continue to refine methodology, products, and costs to further make the acceptance, availability, and use of scAUR^{TM} and VorGAUR^{TM} products more widespread, thus making the products financially viable. AUR has the financial resources to manufacture and provide these products in the future.

INVESTIGATORS PROFILES

Dr. R. L. Simpson, PE - AUR President and Principal Investigator; MSME, PhD, Mechanical Engineering, Stanford University; Past-President American Institute of Aeronautics and Astronautics (AIAA); Past-Chair American Association of Engineering Societies (AAES); Fellow AIAA; Fellow ASME; M. ASCE; international expert on experiments and computations of turbulent separated flows; 40 years experience with metal and composite material structures for air and water experimental models; AUR laboratory experience with various modern precast concrete technologies (SCC, fibers, rebar, mesh wire, coatings and sealants, concrete properties measurements, etc.); over 250 publications, including major sole author review articles.

Dr. Gwibo Byun – Mechanical Engineer; PhD, Virginia Tech; Senior Member AIAA; 12 years experience on experiments on turbulent separated flows; experience in metal structures design and construction; 10 publications.

Mr. Edmund C. Mueller – Civil Engineer; BSCE, MSCE graduate student, Virginia Tech; Experience with concrete and manufacturing processes in bridge construction.

REFERENCES

(1) Jean-Louis Briaud. *Monitoring Scour Critical Bridges*, NCHRP Synthesis 396, 2006.

(2) R. L.Simpson. Turbulent Boundary Layer Separation. Annual Review of Fluid Mechanics, Vol. 21, pp.205 -234, 1989.

(3) R. L. Simpson. Aspects of Turbulent Boundary Layer Separation. Progress in Aerospace Sciences, Vol.32, pp.457 – 521, 1996.

(4) R. L. Simpson. Junction Flows. Annual Review of Fluid Mechanics, Vol. 33, pages 415-443, 2001.

(5) D. M. Sheppard, H. Demir, and B. Melville. *Scour at Wide Piers and Long Skewed Piers*. NCHRP-Report 682, 2011.

(6) R. Ettema, G. Kirkil, and M. Muste. Similitude of large-scale turbulence in experiments on local scour at cylinders. J. Hydraulic Eng., ASCE, Vol. 132, No. 1, pp. 33- 40, Jan. 2006

(7) D. M. Sheppard, M. Odeh, and T.Glasser. Large Scale Clear-Water Local Pier Scour Experiments. J. Hydraulic Eng., ASCE, Vol. 130, pp. 957 -063, 2004.

(8) R. L. Simpson. *Unabridged Report on Full-Scale Prototype Testing and Manufacturing and Installation Plans for New Scour-Vortex-Prevention scAUR^{TM} and VorGAUR^{TM} Products for a Representative Scour-critical Bridge.* AUR, Inc., Internal Report NCHRP-162, July 2013.

(9) P. A. Durbin and B. A. Petterson Reif. *Statistical Theory and Modeling for Turbulent Flows*. John Wiley and Sons, Inc., New York, 2001.

(10) R. L. Simpson. Some Observations on the Structure and Modeling of 3-D Turbulent Boundary Layers and Separated Flow. Invited Plenary Lecture, Turbulent Shear Flow Phenomena-4**,** Williamsburg, Va, June 27-29, 2005.

(11) B. Melville. The Physics of Local Scour at Bridge Piers. Fourth International Conference on Scour and Erosion. Tokyo, Japan, 2008.

(12) Q. Q. Tian, R.L. Simpson, and K. T. Lowe. A laser-based optical approach for measuring scour depth around hydraulic structures. Fifth International Conference on Scour and Erosion, ASCE, San Francisco, Nov. 7-11, 2010.

(13) J. Barlow, W.H. Rae, and A. Pope. *Low-speed Wind Tunnel Testing, 3rd ed.* John Wiley and Sons, New York, pages 353-355, 1999.